



RESEARCH MEMORANDUM

TRANSONIC WIND-TUNNEL INVESTIGATION OF THE EFFECTS
OF A HEATED PROPULSIVE JET ON THE PRESSURE
DISTRIBUTION ALONG A FUSELAGE OVERHANG

By Elden S. Cornette and Donald H. Ward

Langley Aeronautical Laboratory
Langley Field, Va.

NATIONAL ADVISORY COMMITTEE
FOR AERONAUTICS
WASHINGTON

April 4, 1956
Declassified January 20, 1958

NATIONAL ADVISORY COMMITTEE FOR AERONAUTICS

RESEARCH MEMORANDUM

TRANSonic WIND-TUNNEL INVESTIGATION OF THE EFFECTS
OF A HEATED PROPULSIVE JET ON THE PRESSURE
DISTRIBUTION ALONG A FUSELAGE OVERHANG

By Elden S. Cornette and Donald H. Ward

SUMMARY

Pressure-distribution data were obtained on fuselage surfaces which extended downstream of a jet exit and were subject to the influence of a heated propulsive jet. Three fuselage-overhang configurations were investigated at free-stream Mach numbers from 0.80 to 1.10 while jet pressure ratio was varied from 1 to 11 at jet-exit temperature of cold, 800° F, and $1,200^{\circ}$ F.

The data obtained at a model angle of attack of zero, indicated that increasing the jet pressure ratio reduced the pressures on the fuselage undersurface downstream of the jet exit. The effect of increasing jet-exit temperature was to reduce further downstream pressures although the decrement was generally small. Large, negative pressure peaks induced by the jet under the shrouded portion of the overhang were alleviated by moving the overhanging surfaces radially away from the jet axis. Increasing the angle of inclination of the fuselage-overhang produced no significant change in downstream pressures. The fuselage-overhang configuration showed an increase in base annulus drag over the basic body alone but the difference diminished with increasing free-stream Mach number. Pressures measured on the body boattail upstream of the jet exit were increased by the action of the jet.

INTRODUCTION

On some high-speed airplane designs it has been found desirable to locate the large mass of the jet engine forward near the center of gravity of the configuration. This allows the use of shorter air-inlet ducts and may reduce the internal flow losses from this source. At the same time, however, it requires that the jet exit be located at some point ahead of the rear of the configuration in order to maintain short

lengths of tailpipe and reduce tailpipe losses. With this type of design, it then becomes desirable to know the jet effects on that portion of the fuselage which extends downstream of the jet exit.

Reported in reference 1 are the results of an investigation at transonic speeds to determine the effects of a heated propulsive jet on the drag characteristics of a related series of afterbodies. The models used in reference 1 were bodies of revolution which housed a specially designed turbojet simulator. With the addition of a fuselage extension overhanging the jet exit and bearing a vertical tail, this experimental apparatus provided an expedient means of obtaining desired information concerning jet effects on downstream fuselage surfaces which partially surround the jet exhaust. Reported in this paper are the results of an investigation conducted in the Langley 8-foot transonic tunnel to determine the jet effects on the pressure distribution along such a fuselage overhang. The effects of changes in the geometry of the fuselage downstream of the jet exit were investigated by varying the upsweep angle of the fuselage overhang and the radial spacing of the overhang from the jet axis or both.

The investigation was conducted at an angle of attack of 0° and at free-stream Mach numbers of 0.80, 0.90, 1.00, and 1.10. At each point the ratio of jet total pressure to free-stream static pressure was varied at jet total temperatures of cold, $800^\circ F$, and $1,200^\circ F$. While the jet total temperature varied from cold to $1,200^\circ F$, the corresponding ratio of specific heats in the jet varied from 1.40 to 1.35.

SYMBOLS

c_m section pitching-moment coefficient for fuselage overhang,

$$- \frac{L^2}{q_0 d^2} \int_{1.010}^{1.179} (p_l - p_o) \left(\frac{x}{L} - 1 \right) d\left(\frac{x}{L}\right)$$

Δc_m $c_{m,jet\ on} - c_{m,jet\ off}$

c_n section normal-force coefficient for fuselage overhang,

$$\frac{L}{q_0 d} \int_{1.010}^{1.179} (p_l - p_o) d\left(\frac{x}{L}\right)$$

Δc_n $c_{n,jet\ on} - c_{n,jet\ off}$

d	length of projection on jet axis of fuselage overhang, 10.015 in.
D	diameter
h	vertical distance from jet axis to point of intersection of straight-line extension of bottom center line of fuselage overhang and plane of jet exit
H	total pressure
L	length of basic body, 53.011 in.
M	Mach number
p	static pressure
P	pressure coefficient, $\frac{p - p_0}{q_0}$
q	dynamic pressure, $\frac{1}{2}\rho V^2$
r	radius of basic body
R	Reynolds number based on basic-body length
T	total temperature, °F
V	velocity
x	longitudinal distance measured from nose of model, positive rearward
x'	longitudinal distance measured from jet exit, positive rearward
ρ	density
ϕ	angle between bottom center line of fuselage overhang and horizontal

Subscripts:

b	base annulus
j	jet exit
l	local
o	free stream

APPARATUS AND METHODS

Wind Tunnel

This investigation was conducted in the Langley 8-foot transonic tunnel which has a dodecagonal, slotted test section and permitted continuously variable testing through the speed range up to a Mach number of 1.10 for this model. Detailed discussions of the design and calibration of this tunnel have been presented in references 2 and 3. In reference 3 it is shown that the maximum deviation from the indicated free-stream Mach number in the model region is within ± 0.003 . The tunnel is vented to the atmosphere through an air exchange tower which permitted the exhausting of combustion gasses from the model into the stream with no detrimental effects on the characteristics of the stream. The model was mounted in the tunnel by means of two support struts (fig. 1) whose leading edges intersected the body at a point 21.7 inches from the nose and were swept back 45° . The support struts had a chord of 11.25 inches and an NACA 65-010 airfoil section measured parallel to the airstream.

Model

The model used in this investigation consisted of a body of revolution at the rear of which was mounted a fuselage overhang bearing a vertical tail. The ordinates defining the basic body of revolution are given in figure 2. This body was the same as that reported in reference 1. The body was cut off at the 53.011-inch station to provide an exit for the jet and this resulted in a basic body fineness ratio of 10.6. The boattail angle of the body was 16° , the base diameter was 1.672 inches, and the ratio of jet diameter to base diameter was 0.742.

Three fuselage-overhang configurations were used in this investigation. The geometry of the configurations, including the vertical tail, is shown in figure 3 where a table of coordinates for typical cross sections is given. The three overhangs differed only in the angle of inclination of the base line to the horizontal ϕ , the vertical spacing of the bottom center line above the jet axis h , or both. The vertical tail, whose root section was located at the level $z = 3.352$ inches, consisted of an NACA 65A007 airfoil section oriented parallel to the body center line.

Inside the body of the model was located a turbojet simulator which burned a mixture of ethylene and air. The products of combustion were exhausted through a sonic nozzle at the base of the body. The pressure and temperature range that would be experienced by a non-afterburning

turbojet exhaust was covered. The details of the design and installation of the turbojet simulator are given in reference 1. A photograph of the model mounted in the tunnel is presented in figure 4.

Tests

In this investigation, the body of revolution alone, as well as the three body-tail combinations, were tested at an angle of attack of 0° and at free-stream Mach numbers of 0.80, 0.90, 1.00, and 1.10. At each test Mach number, the ratio of jet total pressure to free-stream static pressure was varied from a jet-off condition to 11 or to the maximum attainable at jet temperatures of cold, $800^\circ F$, and $1,200^\circ F$. The term "cold" flow is used herein to define the temperature of the air coming from the source, normally 75° to 80° , and corresponds to a fuel-air ratio of 0. The jet pressure ratio for a jet-off, or no-flow, condition was assigned a value of 1 in the presentation of the results. The Reynolds number based on basic-body length varied from 16.0×10^6 to 17.4×10^6 . (See fig. 5.)

Measurements

The locations of static-pressure orifices on the three fuselage overhangs and base annulus are given in figure 6. At each test point, fuselage-overhang pressure distribution and base-annulus pressures were photographically recorded from multiple-tube manometers. The accuracy of the pressure coefficients determined therefrom and reported herein is estimated to be ± 0.005 .

Internal instrumentation consisted of a shielded chromel-alumel thermocouple mounted in the converging nozzle near the jet-exit station for measuring jet temperature, and a calibrated total-pressure probe mounted in the combustor. The total-pressure probe was referenced to a static-pressure orifice on the tunnel wall for the determination of jet pressure ratio. Jet temperature and pressure ratio were photographically recorded by a camera synchronized with that used to record pressure-distribution data. The accuracy of the jet pressure ratios reported herein is estimated to be ± 0.02 .

RESULTS AND DISCUSSION

Presented in table I are the pressure-coefficient results for the row of pressure orifices located along the bottom center line of each fuselage overhang and extending downstream of the jet exit (orifices 12

to 29, fig. 6). These pressure distributions were examined to determine the effects of such test variables as jet pressure ratio, jet-exit temperature, free-stream Mach number, and fuselage-overhang geometry. In order to illustrate the general shape of the pressure-distribution curves, a jet-off condition for the overhang configuration with $\phi = 7^\circ$ and $h/D_j = 0.855$ was selected. These pressure distributions are plotted in figure 7 for the range of free-stream Mach numbers investigated. These curves represent the general shape of the pressure distributions at the various test Mach numbers although they are altered by jet action, particularly at the higher jet pressure ratios, and to a lesser extent by jet temperature and overhang geometry. It can be seen that, with the jet off, large positive pressures were measured immediately downstream of the jet exit for all stream Mach numbers. A rather rapid decrease in pressure with distance downstream to approximately 50 percent of the overhang length was observed. At this point the pressures tended to level off at near stream values with the exception of the case in which the external flow was supersonic. For this case the pressure reduction continued the entire length of the overhang resulting in appreciable negative pressures acting on the rear portion. In figure 8, the jet-off pressure distribution along the fuselage overhang is compared with the jet-on pressure distribution for a jet pressure ratio of 11 and a jet-exit temperature of $1,200^\circ F$.

Presented in figure 9 are curves of the increment in pressure coefficient due to the influence of the jet. Since it was possible to obtain higher jet pressure ratios with a heated jet, a jet temperature of $1,200^\circ F$ was selected for this illustration. The increment in pressure coefficient shown in figure 9 represents the difference between the jet operating at $1,200^\circ F$ and the jet off. It can be seen that, in general, the effect of operating the jet was to reduce the pressures acting on the overhang. At the higher jet pressure ratios, very low pressures were induced just downstream of the exit on the overhang configuration whose surface was located nearest to the jet axis. (See figs. 9(a) and 9(b).) The effect of increasing free-stream Mach number at a constant jet pressure ratio was to reduce the negative pressure peaks. By increasing the radial spacing of the overhang surface from $h/D_j = 0.855$ to $h/D_j = 1.040$, a considerable reduction in the negative pressure peaks was realized. (See fig. 9(c).) Since the jet was exhausted through a sonic nozzle and considerable jet expansion occurred as the flow left the nozzle, it is believed that these very low pressures were the result of the jet boundary being very near, or attached to, the surface of the overhang and the jet aspirating the orifices in the region just downstream of the exit.

Shown in figure 10 are schlieren photographs of the jet flow with and without the overhang mounted on the afterbody. Due to the mechanical arrangement of the schlieren apparatus and the fact that the model was mounted on its side in the wind tunnel, only a bottom view of the jet

in the presence of the overhang was obtained. The compression waves shown intersecting with the afterbody upstream of the jet exit originated at the juncture between the support struts and the body and were subsequently reflected from the tunnel boundary to the afterbody. This wave was again reflected from the afterbody as can be seen in the photographs. At a free-stream Mach number of 1.10 the absolute values of the pressures measured downstream would be expected to be altered by the reflected disturbance. An indication of the order of magnitude of this change can be found in reference 3. Examination of pressure distributions along the body and schlieren photographs obtained in the region of the rear of the body indicated no evidence of flow separation due to this disturbance. Consequently the magnitude of the jet effects was considered to be essentially unaffected. In figure 10(b) can be seen the characteristic Riemann wave (ref. 4) which occurs in the jet at higher jet pressure ratios. Shown in figure 10(c) is a sketch of the side profile of the fuselage overhang ($\phi = 7^\circ$, $h/D_j = 0.855$) drawn to the same scale as the accompanying schlieren photograph. The approximate jet boundary was scaled from the schlieren photograph and is shown as a dashed line in the sketch. It can be seen that, with an axially symmetrical jet at a high jet pressure ratio, the jet flow would be near or attached to the surface of the overhang over a small region and the extremely low pressures could be expected to produce large skin load differentials. High skin temperatures would also occur in this region.

The effect of increasing the upsweep angle ϕ of the fuselage overhang from 7° to 10° was found to be insignificant. Examination of pressure-distribution curves indicated a small increase in pressure coefficient for the orifices located near the downstream tip of the overhang when the upsweep angle was increased to 10° . Pressures near the jet exit were essentially unaffected.

The effect of increasing the jet-exit temperature is shown in figure 11 where the increment in pressure coefficient due to temperature is plotted for a constant free-stream Mach number and jet pressure ratio. Due to a limited air supply, it was not possible to obtain the higher jet pressure ratios with a cold jet. For the higher jet pressure ratios, it was therefore necessary to show the temperature effect as the difference between the jet operating at $1,200^\circ F$ and $800^\circ F$. For jet pressure ratios of 5 or less, the effect of jet temperature is generally confined to the region near the jet exit. Increasing jet temperature at the higher jet pressure ratios results generally in a reduction of the pressures on the overhang but the effects are somewhat erratic. At a constant jet pressure ratio, increasing the jet-exit temperature resulted in small changes in the value of the ratio of specific heats in the jet and, consequently, in small changes in the static pressure at the jet exit.

For each test condition the pressure coefficients presented in table I were plotted and integrated. The results of the integrations are presented in the form of an increment in section normal-force coefficient (fig. 12) and section pitching-moment coefficient (fig. 13) plotted against jet pressure ratio. The length of the overhang downstream of the jet exit (10.015 in.) was used to reduce the data to coefficient form. The pitch center was arbitrarily taken as the point on the jet axis in the plane of the jet exit and a nose-up pitching moment was designated positive. Figure 12 shows that the integrated pressure load on the fuselage overhang was reduced by an increase in jet pressure ratio for all three configurations and at all test Mach numbers. The effect of increasing jet-exit temperature on the integrated pressure loads is shown in figure 14. It can be seen that increasing jet-exit temperature produced no significant change in the increment in section normal-force coefficient due to the jet until the higher jet pressure ratios were reached. Increasing h/D_j from 0.855 to 1.040 produced a slight increase in normal force with temperature at a free-stream Mach number of 1.10. No explanation for this deviation is available. It can be seen that increasing the upsweep angle ϕ of the fuselage overhang from 7° to 10° produced little change in the temperature effects.

Figure 13 shows that the effect of the jet was to produce a nose-up increment in section pitching-moment coefficient in all cases. This was due to the decrement in normal force produced by the jet. Increasing the jet temperature or overhang spacing from the jet axis produced essentially no change in the pitching-moment increment due to the jet. Increasing the angle of upsweep of the overhang from 7° to 10° produced a small nose-down increment in pitching moment in all cases. This was due to a slight rearward shift of the local center-of-pressure location.

The effect of jet pressure ratio and fuselage-overhang geometry on the base-annulus pressure coefficient is illustrated in figure 15. Pressure coefficients were calculated using pressures measured at orifices 30 and 31 (fig. 6) for the three overhang configurations as well as the basic body alone. Figure 15 shows that the base pressure coefficient was positive for all configurations and increased with stream Mach number at subsonic speeds. A decrease was observed when the external stream became supersonic. Adding an overhang to the basic fuselage produced a reduction in base-annulus pressure coefficient (increase in base-annulus drag). This reduction was greatest at subsonic speeds and diminished with increasing free-stream Mach number. It appears that, in the case of the basic body alone, at a jet-exit temperature of $1,200^\circ F$, the jet itself aspirated the base-annulus region up to a jet pressure ratio of approximately 3. At this point, the jet spreading became sufficient to cause increased outward turning and compression of the external stream. The consequent pressure buildup was felt in the annulus region and a subsequent increase in base-annulus pressure with jet pressure ratio

resulted. The effect of adding an overhang to the fuselage was to allow the jet to continue to aspirate the annulus region to a jet pressure ratio of about 5 to 7 before the jet spread became sufficient to cause an increase in base-annulus pressure. Figure 15 also shows that increasing jet-exit temperature from cold to $1,200^{\circ}$ F produced a small increase in base-annulus pressure coefficient and increased the variation between the pressures measured at orifices 30 and 31.

The effect of the jet on the pressures measured upstream of the exit (orifices 1 to 9, fig. 6), and on the lip of the overhang (orifices 10 and 11), is shown in figure 16. It can be seen that increasing jet pressure ratio produced an increase in the pressures acting on the body boattail even at supersonic speeds. This favorable jet effect is probably due to positive pressures in the annulus region feeding upstream through the subsonic boundary layer which surrounds the body boattail. The extent to which the favorable pressures are felt upstream indicates that a sizable reduction in boattail drag due to jet action is realized for this type of configuration.

SUMMARY OF RESULTS

A transonic wind-tunnel investigation was conducted to determine the effects of a heated propulsive jet on the pressure distribution along a fuselage overhang. Three overhang configurations were tested at zero angle of attack and at free-stream Mach numbers of 0.80, 0.90, 1.00, and 1.10. The jet-exit temperature was varied from cold to $1,200^{\circ}$ F through a range of jet total-pressure ratios from 1 to 11. The following results were obtained:

1. The general effect of increasing jet pressure ratio was to reduce the pressures on the shrouded portion of the fuselage undersurface downstream of the jet exit.
2. The effect of increasing jet-exit temperature was to reduce further downstream pressures although the decrement was generally small at moderate pressure ratios.
3. Large negative pressure peaks induced by the jet at high pressure ratios were reduced considerably by moving the overhanging surfaces radially away from the jet axis. Increasing the angle of inclination of the fuselage overhang produced no significant change in downstream pressures.
4. An increase in base-annulus drag was incurred by the addition of a fuselage overhang to the basic body. This increase, however, diminished with increasing free-stream Mach number.

5. Pressures measured on the body boattail upstream of the jet exit were increased by the action of the jet.

Langley Aeronautical Laboratory,
National Advisory Committee for Aeronautics,
Langley Field, Va., January 11, 1956.

REFERENCES

1. Henry, Beverly Z., Jr., and Cahn, Maurice S.: Preliminary Results of an Investigation at Transonic Speeds To Determine the Effects of a Heated Propulsive Jet on the Drag Characteristics of a Related Series of Afterbodies. NACA RM L55A24a, 1955.
2. Wright, Ray H., and Ritchie, Virgil S.: Characteristics of a Transonic Test Section With Various Slot Shapes in the Langley 8-Foot High-Speed Tunnel. NACA RM L51H10, 1951.
3. Ritchie, Virgil S., and Pearson, Albin O.: Calibration of the Slotted Test Section of the Langley 8-Foot Transonic Tunnel and Preliminary Experimental Investigation of Boundary-Reflected Disturbances. NACA RM L51K14, 1952.
4. Love, Eugene S., and Grigsby, Carl E.: Some Studies of Axisymmetric Free Jets Exhausting From Sonic and Supersonic Nozzles Into Still Air and Into Supersonic Streams. NACA RM L54L31, 1955.

TABLE I.- FUSELAGE-OVERHANG PRESSURE COEFFICIENTS

(a) $h/D_J = 0.855$; $\phi = 7^\circ$; $M_\infty = 0.80$

Jet-exit temperature, T_J , °F	Orifice location, x'/D_J	Orifice location, x/L	Pressure coefficient for jet pressure ratio H_J/p_∞ of -						
			Jet off	2	3	5	7	9	11
80	0.428	1.010	0.106	0.083	0.074	0.065	-----	-----	-----
	.812	1.019	.137	.142	.113	.078	-----	-----	-----
	1.197	1.028	.167	.206	.186	.119	-----	-----	-----
	1.625	1.038	.172	.178	.186	.170	-----	-----	-----
	2.009	1.047	-----	-----	-----	-----	-----	-----	-----
	2.437	1.057	.141	.113	.117	.113	-----	-----	-----
	2.822	1.066	.104	.069	.063	.049	-----	-----	-----
	3.206	1.075	.084	.049	.051	.047	-----	-----	-----
	3.634	1.085	.062	.035	.031	.069	-----	-----	-----
	4.019	1.094	.044	.018	.007	.026	-----	-----	-----
	4.446	1.104	.029	.009	.004	-.020	-----	-----	-----
	4.831	1.113	.031	.013	.005	-.013	-----	-----	-----
	5.216	1.122	.027	.013	.008	.015	-----	-----	-----
	5.643	1.132	.033	.022	.021	.044	-----	-----	-----
	6.028	1.141	.024	.014	.009	.023	-----	-----	-----
	6.455	1.151	.018	.010	.006	-.001	-----	-----	-----
	6.840	1.160	.036	.032	.030	.022	-----	-----	-----
	7.652	1.179	-.039	-.018	-.020	-.006	-----	-----	-----
800	0.428	1.010	-----	0.099	0.089	0.076	0.066	0.085	-----
	.812	1.019	-----	.149	.129	.082	.005	-.077	-----
	1.197	1.028	-----	.199	.191	.112	.039	-.140	-----
	1.625	1.038	-----	.177	.180	.154	.113	.048	-----
	2.009	1.047	-----	-----	-----	-----	-----	-----	-----
	2.437	1.057	-----	.115	.120	.107	.125	.185	-----
	2.822	1.066	-----	.073	.071	.046	.046	.078	-----
	3.206	1.075	-----	.054	.053	.051	.022	.024	-----
	3.634	1.085	-----	.038	.033	.062	.013	.009	-----
	4.019	1.094	-----	.021	.016	.017	.025	.013	-----
	4.446	1.104	-----	.010	.004	-.024	.032	.004	-----
	4.831	1.113	-----	.015	.008	-.007	.011	.053	-----
	5.216	1.122	-----	.016	.013	.020	-.009	.038	-----
	5.643	1.132	-----	.023	.021	.039	.001	.013	-----
	6.028	1.141	-----	.016	.012	.011	.008	-.007	-----
	6.455	1.151	-----	.012	.009	-.006	.018	-.012	-----
	6.840	1.160	-----	.032	.030	.026	.045	.021	-----
	7.652	1.179	-----	-.014	-.018	-.012	-.007	.023	-----
1,200	0.428	1.010	-----	0.100	0.090	0.084	0.084	0.118	-----
	.812	1.019	-----	.145	.123	.088	-.019	-.053	-----
	1.197	1.028	-----	.187	.184	.108	.022	-.258	-----
	1.625	1.038	-----	.177	.178	.128	.096	-.042	-----
	2.009	1.047	-----	-----	-----	-----	-----	-----	-----
	2.437	1.057	-----	.117	.118	.107	.137	.177	-----
	2.822	1.066	-----	.074	.073	.047	.049	.097	-----
	3.206	1.075	-----	.053	.055	.040	.020	.020	-----
	3.634	1.085	-----	.036	.034	.055	.012	.008	-----
	4.019	1.094	-----	.025	.022	.035	.028	.024	-----
	4.446	1.104	-----	.007	.004	-.017	.030	.001	-----
	4.831	1.113	-----	.012	.010	-.010	.015	.052	-----
	5.216	1.122	-----	.013	.011	.010	-.007	.040	-----
	5.643	1.132	-----	.020	.021	.038	-.003	.012	-----
	6.028	1.141	-----	.013	.012	.016	-.003	-.011	-----
	6.455	1.151	-----	.008	.009	-.003	.011	-.018	-----
	6.840	1.160	-----	.030	.031	.023	.043	.019	-----
	7.652	1.179	-----	-.016	-.015	-.009	-.009	.012	-----

TABLE I.- FUSELAGE-OVERHANG PRESSURE COEFFICIENTS - Continued

(b) $h/D_j = 0.855$; $\phi = 10^\circ$; $M_\infty = 0.80$

Jet-exit temperature, T_j , °F	Orifice location, x'/D_j	Orifice location, x/L	Pressure coefficient for jet pressure ratio H_j/p_0 of -					
			Jet off	2	3	5	7	9
80	0.428	1.010	0.111	0.075	0.063	0.051	-----	-----
	.812	1.019	.146	.145	.117	.079	-----	-----
	1.197	1.028	-----	-----	-----	-----	-----	-----
	1.625	1.038	.174	.184	.190	.153	-----	-----
	2.009	1.047	-----	-----	-----	-----	-----	-----
	2.437	1.057	.131	.110	.115	.079	-----	-----
	2.822	1.066	.100	.072	.075	.037	-----	-----
	3.206	1.075	.076	.048	.050	.032	-----	-----
	3.634	1.085	.059	.035	.033	.037	-----	-----
	4.019	1.094	.034	.009	.004	-.004	-----	-----
	4.446	1.104	.024	.001	-.002	-.026	-----	-----
	4.831	1.113	.033	.019	.016	-.003	-----	-----
	5.216	1.122	.034	.025	.022	.016	-----	-----
	5.643	1.132	.039	.032	.028	.032	-----	-----
	6.028	1.141	.032	.029	.025	.026	-----	-----
	6.455	1.151	.045	.045	.042	.037	-----	-----
	6.840	1.160	.051	.055	.052	.049	-----	-----
	7.652	1.179	.045	.052	.049	.057	-----	-----
800	0.428	1.010	-----	0.085	0.075	0.063	0.066	0.064
	.812	1.019	-----	.151	.137	.080	.051	.020
	1.197	1.028	-----	-----	-----	-----	-----	-----
	1.625	1.038	-----	.179	.180	.159	.092	.067
	2.009	1.047	-----	-----	-----	-----	-----	-----
	2.437	1.057	-----	.105	.107	.073	.080	.122
	2.822	1.066	-----	.068	.070	.035	.021	.053
	3.206	1.075	-----	.043	.043	.031	.002	-.004
	3.634	1.085	-----	.032	.030	.030	.001	.004
	4.019	1.094	-----	.008	.004	-.013	-.003	-.011
	4.446	1.104	-----	.001	-.002	-.030	-.003	-.007
	4.831	1.113	-----	.017	.014	-.003	-.002	.028
	5.216	1.122	-----	.021	.020	.017	-.007	.019
	5.643	1.132	-----	.027	.025	.025	.004	.011
	6.028	1.141	-----	.027	.022	.015	.018	.004
	6.455	1.151	-----	.041	.038	.033	.048	.032
	6.840	1.160	-----	.053	.050	.050	.063	.056
	7.652	1.179	-----	.050	.047	.052	.053	.067
1,200	0.428	1.010	-----	0.084	0.069	0.068	0.071	0.080
	.812	1.019	-----	.143	.117	.080	.053	.015
	1.197	1.028	-----	.171	.178	.090	.004	-.100
	1.625	1.038	-----	.170	.173	.142	.085	.047
	2.009	1.047	-----	-----	-----	-----	-----	-----
	2.437	1.057	-----	.105	.103	.071	.091	.104
	2.822	1.066	-----	.071	.067	.029	.029	.065
	3.206	1.075	-----	.046	.043	.021	.006	.001
	3.634	1.085	-----	.031	.027	.023	.003	-.003
	4.019	1.094	-----	.007	.002	-.008	-.004	-.015
	4.446	1.104	-----	-.002	-.005	-.028	-.004	-.013
	4.831	1.113	-----	.017	.014	-.005	.005	.027
	5.216	1.122	-----	.021	.017	.010	-.002	.024
	5.643	1.132	-----	.027	.023	.025	.005	.013
	6.028	1.141	-----	.030	.024	.024	.018	.010
	6.455	1.151	-----	.040	.038	.035	.045	.031
	6.840	1.160	-----	.053	.050	.050	.060	.052
	7.652	1.179	-----	.049	.048	.054	.053	.066

TABLE I.- FUSELAGE-OVERHANG PRESSURE COEFFICIENTS - Continued

(c) $h/D_j = 1.040$; $\phi = 7^\circ$; $M_\infty = 0.80$

Jet-exit température, $T_j, {}^{\circ}\text{F}$	Orifice location, x'/D_j	Orifice location, x/L	Pressure coefficient for jet pressure ratio H_j/p_0 of -						
			Jet off	2	3	5	7	9	11
80	0.428	1.010	0.113	0.086	0.071	0.076	-----	-----	-----
	.812	1.019	.133	.154	.143	.095	-----	-----	-----
	1.197	1.028	.150	.217	.220	.135	-----	-----	-----
	1.625	1.038	.149	.191	.194	.165	-----	-----	-----
	2.009	1.047	.145	.171	.173	.165	-----	-----	-----
	2.437	1.057	.123	.117	.114	.108	-----	-----	-----
	2.822	1.066	.097	.079	.077	.065	-----	-----	-----
	3.206	1.075	.073	.054	.050	.056	-----	-----	-----
	3.634	1.085	.056	.038	.033	.055	-----	-----	-----
	4.019	1.094	.039	.024	.019	.023	-----	-----	-----
	4.446	1.104	.029	.013	.005	-.007	-----	-----	-----
	4.831	1.113	.030	.019	.012	.004	-----	-----	-----
	5.216	1.122	.025	.017	.010	.018	-----	-----	-----
	5.643	1.132	.034	.029	.024	.042	-----	-----	-----
	6.028	1.141	.035	.031	.027	.033	-----	-----	-----
	6.455	1.151	.029	.025	.020	.015	-----	-----	-----
	6.840	1.160	.038	.041	.036	.036	-----	-----	-----
	7.652	1.179	-.070	-.074	-.070	-.068	-----	-----	-----
800	0.428	1.010	-----	0.091	0.079	0.087	0.081	0.091	-----
	.812	1.019	-----	.143	.127	.100	.089	.069	-----
	1.197	1.028	-----	.200	.197	.130	.100	.043	-----
	1.625	1.038	-----	.177	.175	.147	.112	.038	-----
	2.009	1.047	-----	.161	.157	.153	.127	.071	-----
	2.437	1.057	-----	.110	.103	.105	.100	.101	-----
	2.822	1.066	-----	.076	.068	.065	.054	.071	-----
	3.206	1.075	-----	.053	.043	.053	.029	.021	-----
	3.634	1.085	-----	.034	.027	.050	.020	-.001	-----
	4.019	1.094	-----	.023	.014	.021	.023	.001	-----
	4.446	1.104	-----	.010	.003	-.002	.021	.004	-----
	4.831	1.113	-----	.015	.009	.006	.014	.033	-----
	5.216	1.122	-----	.016	.009	.022	.000	.029	-----
	5.643	1.132	-----	.026	.020	.038	.010	.019	-----
	6.028	1.141	-----	.028	.022	.031	.024	.014	-----
	6.455	1.151	-----	.026	.018	.019	.034	.014	-----
	6.840	1.160	-----	.038	.032	.035	.054	.029	-----
	7.652	1.179	-----	-.066	-.064	-.061	-.061	-.029	-----
1,200	0.428	1.010	-----	0.092	0.080	0.100	0.096	0.109	-----
	.812	1.019	-----	.138	.121	.109	.097	.079	-----
	1.197	1.028	-----	.191	.202	.134	.098	.049	-----
	1.625	1.038	-----	.179	.186	.152	.108	.037	-----
	2.009	1.047	-----	.162	.165	.155	.128	.068	-----
	2.437	1.057	-----	.111	.110	.108	.104	.096	-----
	2.822	1.066	-----	.076	.072	.061	.054	.077	-----
	3.206	1.075	-----	.050	.046	.045	.020	.024	-----
	3.634	1.085	-----	.034	.029	.048	.013	.001	-----
	4.019	1.094	-----	.018	.013	.022	.020	.003	-----
	4.446	1.104	-----	.005	.001	-.014	.020	.009	-----
	4.831	1.113	-----	.014	.009	-.002	.017	.033	-----
	5.216	1.122	-----	.014	.010	.014	.001	.029	-----
	5.643	1.132	-----	.023	.018	.034	.006	.020	-----
	6.028	1.141	-----	.026	.023	.030	.019	.018	-----
	6.455	1.151	-----	.026	.024	.022	.034	.018	-----
	6.840	1.160	-----	.036	.030	.032	.048	.030	-----
	7.652	1.179	-----	-.070	-.066	-.068	-.064	-.030	-----

TABLE I.- FUSELAGE-OVERHANG PRESSURE COEFFICIENTS - Continued

(d) $h/D_j = 0.855$; $\phi = 7^\circ$; $M_\infty = 0.90$

Jet-exit temperature, T_j , $^{\circ}\text{F}$	Orifice location, x'/D_j	Orifice location, x/L	Pressure coefficient for jet pressure ratio H_j/p_0 of -						
			Jet off	2	3	5	7	9	11
80	0.428	1.010	0.117	0.106	0.102	0.094	-----	-----	-----
	.812	1.019	.148	.156	.134	.108	-----	-----	-----
	1.197	1.028	.176	.209	.198	.141	-----	-----	-----
	1.625	1.038	.179	.186	.195	.182	-----	-----	-----
	2.009	1.047	-----	-----	-----	-----	-----	-----	-----
	2.437	1.057	.147	.116	.123	.119	-----	-----	-----
	2.822	1.066	.108	.064	.059	.032	-----	-----	-----
	3.206	1.075	.083	.046	.049	.033	-----	-----	-----
	3.634	1.085	.058	.025	.024	.065	-----	-----	-----
	4.019	1.094	.037	.004	-.006	.025	-----	-----	-----
	4.446	1.104	.018	-.006	-.006	-.043	-----	-----	-----
	4.831	1.113	.020	-.002	-.005	-.051	-----	-----	-----
	5.216	1.122	.018	.001	-.003	-.020	-----	-----	-----
	5.643	1.132	.025	.014	.016	.035	-----	-----	-----
	6.028	1.141	.019	.009	.009	.034	-----	-----	-----
	6.455	1.151	.016	.007	.003	.004	-----	-----	-----
	6.840	1.160	.035	.033	.033	.011	-----	-----	-----
	7.652	1.179	-.040	-.016	-.016	-.001	-----	-----	-----
800	0.428	1.010	-----	0.117	0.112	0.103	0.096	0.116	-----
	.812	1.019	-----	.159	.146	.112	.039	-.028	-----
	1.197	1.028	-----	.202	.196	.136	.061	-.093	-----
	1.625	1.038	-----	.180	.188	.171	.120	.036	-----
	2.009	1.047	-----	-----	-----	-----	-----	-----	-----
	2.437	1.057	-----	.116	.119	.109	.132	.176	-----
	2.822	1.066	-----	.071	.070	.038	.044	.095	-----
	3.206	1.075	-----	.047	.044	.046	.007	.017	-----
	3.634	1.085	-----	.029	.021	.062	-.015	-.017	-----
	4.019	1.094	-----	.008	.005	.006	-.002	-.013	-----
	4.446	1.104	-----	-.005	-.013	-.053	.025	-.038	-----
	4.831	1.113	-----	-.001	-.007	-.043	.012	.018	-----
	5.216	1.122	-----	.001	.000	.003	-.019	.054	-----
	5.643	1.132	-----	.011	.011	.039	-.025	.023	-----
	6.028	1.141	-----	.008	.006	.013	-.021	-.010	-----
	6.455	1.151	-----	.007	.005	-.017	-.002	-.021	-----
	6.840	1.160	-----	.030	.029	.012	.046	.003	-----
	7.652	1.179	-----	-.016	-.020	-.004	.001	.028	-----
1,200	0.428	1.010	-----	0.117	0.112	0.110	0.110	0.142	-----
	.812	1.019	-----	.154	.140	.115	.031	-.018	-----
	1.197	1.028	-----	.192	.191	.129	.047	-.152	-----
	1.625	1.038	-----	.182	.181	.148	.101	-.049	-----
	2.009	1.047	-----	-----	-----	-----	-----	-----	-----
	2.437	1.057	-----	.117	.123	.109	.138	.154	-----
	2.822	1.066	-----	.071	.072	.041	.050	.121	-----
	3.206	1.075	-----	.047	.049	.028	.008	.018	-----
	3.634	1.085	-----	.027	.023	.045	-.011	-.019	-----
	4.019	1.094	-----	.012	.009	.030	-.002	-.007	-----
	4.446	1.104	-----	-.009	-.010	-.032	.018	-.035	-----
	4.831	1.113	-----	-.002	-.006	-.038	.016	.011	-----
	5.216	1.122	-----	-.001	-.002	-.017	-.014	.053	-----
	5.643	1.132	-----	.009	.010	.025	-.020	.028	-----
	6.028	1.141	-----	.004	.004	.022	-.025	-.013	-----
	6.455	1.151	-----	.004	.005	-.001	-.007	-.020	-----
	6.840	1.160	-----	.027	.030	.015	.042	.006	-----
	7.652	1.179	-----	-.017	-.013	-.005	.004	.017	-----

TABLE I.- FUSELAGE-OVERHANG PRESSURE COEFFICIENTS - Continued

(e) $h/D_j = 0.855$; $\phi = 10^\circ$; $M_\infty = 0.90$

Jet-exit temperature, T_j , °F	Orifice location, x'/D_j	Orifice location, x/L	Pressure coefficient for jet pressure ratio H_j/p_0 of -						
			Jet off	2	3	5	7	9	11
80	0.428	1.010	0.121	0.097	0.091	0.084	-----	-----	-----
	.812	.153	.153	.135	.108	-----	-----	-----	-----
	1.197	-----	-----	-----	-----	-----	-----	-----	-----
	1.625	1.038	.182	.189	.198	.166	-----	-----	-----
	2.009	1.047	-----	-----	-----	-----	-----	-----	-----
	2.437	1.057	.137	.111	.117	.083	-----	-----	-----
	2.822	1.066	.103	.068	.072	.032	-----	-----	-----
	3.206	1.075	.075	.059	.044	.027	-----	-----	-----
	3.634	1.085	.055	.023	.022	.035	-----	-----	-----
	4.019	1.094	.026	-.006	-.008	-.013	-----	-----	-----
	4.446	1.104	.014	-.016	-.016	-.049	-----	-----	-----
	4.831	1.113	.021	.006	.001	-.031	-----	-----	-----
	5.216	1.122	.025	.012	.013	-.001	-----	-----	-----
	5.643	1.132	.031	.024	.022	.029	-----	-----	-----
	6.028	1.141	.028	.024	.021	.028	-----	-----	-----
	6.455	1.151	.047	.043	.044	.034	-----	-----	-----
	6.840	1.160	.054	.058	.058	.045	-----	-----	-----
	7.652	1.179	.048	.054	.055	.062	-----	-----	-----
800	0.428	1.010	-----	0.109	0.101	0.093	0.096	0.105	-----
	.812	-----	-----	.161	.155	.113	.089	.061	-----
	1.197	1.028	-----	-----	-----	-----	-----	-----	-----
	1.625	1.038	-----	.184	.192	.170	.124	.066	-----
	2.009	1.047	-----	-----	-----	-----	-----	-----	-----
	2.437	1.057	-----	.108	.112	.078	.093	.128	-----
	2.822	1.066	-----	.068	.071	.030	.027	.061	-----
	3.206	1.075	-----	.040	.039	.028	-.003	-.013	-----
	3.634	1.085	-----	.022	.022	.029	-.012	-.017	-----
	4.019	1.094	-----	-.006	-.006	-.022	-.015	-.035	-----
	4.446	1.104	-----	-.013	-.015	-.054	-.007	-.035	-----
	4.831	1.113	-----	.003	.004	-.027	-.004	.017	-----
	5.216	1.122	-----	.008	.009	.005	-.016	.027	-----
	5.643	1.132	-----	.019	.019	.025	-.009	.013	-----
	6.028	1.141	-----	.022	.022	.017	.007	-.001	-----
	6.455	1.151	-----	.041	.043	.029	.047	.022	-----
	6.840	1.160	-----	.055	.057	.049	.070	.050	-----
	7.652	1.179	-----	.054	.054	.060	.062	.074	-----
1,200	0.428	1.010	-----	0.105	0.099	0.096	0.104	0.112	-----
	.812	1.019	-----	.155	.138	.112	.087	.052	-----
	1.197	1.028	-----	.179	.187	.119	.037	-.065	-----
	1.625	1.038	-----	.176	.182	.156	.107	.041	-----
	2.009	1.047	-----	-----	-----	-----	-----	-----	-----
	2.437	1.057	-----	.107	.111	.079	.099	.106	-----
	2.822	1.066	-----	.069	.067	.029	.030	.072	-----
	3.206	1.075	-----	.041	.041	.015	-.003	-.008	-----
	3.634	1.085	-----	.022	.021	.020	-.014	-.026	-----
	4.019	1.094	-----	-.006	-.008	-.013	-.021	-.038	-----
	4.446	1.104	-----	-.015	-.017	-.041	-.010	-.041	-----
	4.831	1.113	-----	.001	.002	-.027	-.001	.008	-----
	5.216	1.122	-----	.008	.008	-.005	-.013	.025	-----
	5.643	1.132	-----	.017	.017	.020	-.011	.016	-----
	6.028	1.141	-----	.022	.023	.025	.006	.005	-----
	6.455	1.151	-----	.038	.039	.035	.038	.023	-----
	6.840	1.160	-----	.052	.055	.048	.065	.045	-----
	7.652	1.179	-----	.050	.054	.059	.064	.070	-----

TABLE I.- FUSELAGE-OVERHANG PRESSURE COEFFICIENTS - Continued

(f) $h/D_j = 1.040$; $\phi = 7^\circ$; $M_\infty = 0.90$

Jet-exit temperature, T_j , °F	Orifice location, x'/D_j	Orifice location, x/L	Pressure coefficient for jet pressure ratio H_j/p_0 of -						
			Jet off	2	3	5	7	9	11
80	0.428	1.010	0.124	0.105	0.094	0.102	-----	-----	-----
	.812	1.019	.143	.157	.150	.119	-----	-----	-----
	1.197	1.028	.160	.219	.223	.149	-----	-----	-----
	1.625	1.038	.159	.197	.203	.172	-----	-----	-----
	2.009	1.047	.154	.178	.181	.174	-----	-----	-----
	2.437	1.057	.130	.122	.120	.112	-----	-----	-----
	2.822	1.066	.103	.081	.079	.059	-----	-----	-----
	3.206	1.075	.074	.048	.045	.049	-----	-----	-----
	3.634	1.085	.053	.027	.023	.054	-----	-----	-----
	4.019	1.094	.033	.010	.007	.015	-----	-----	-----
	4.446	1.104	.021	-.003	-.012	-.034	-----	-----	-----
	4.831	1.113	.019	.005	-.002	-.029	-----	-----	-----
	5.216	1.122	.018	.004	-.002	-.003	-----	-----	-----
	5.643	1.132	.026	.020	.014	.040	-----	-----	-----
	6.028	1.141	.030	.025	.022	.039	-----	-----	-----
	6.455	1.151	.030	.022	.018	.012	-----	-----	-----
	6.840	1.160	.040	.043	.039	.026	-----	-----	-----
	7.652	1.179	-.071	-.078	-.075	-.063	-----	-----	-----
800	0.428	1.010	-----	0.117	0.105	0.106	0.107	0.112	-----
	.812	1.019	-----	.155	.146	.117	.115	.090	-----
	1.197	1.028	-----	.204	.203	.143	.121	.070	-----
	1.625	1.038	-----	.186	.191	.158	.132	.066	-----
	2.009	1.047	-----	.167	.170	.158	.143	.091	-----
	2.437	1.057	-----	.117	.113	.102	.110	.105	-----
	2.822	1.066	-----	.080	.073	.058	.055	.069	-----
	3.206	1.075	-----	.050	.044	.048	.018	.014	-----
	3.634	1.085	-----	.029	.024	.041	.001	-.016	-----
	4.019	1.094	-----	.014	.005	.004	.012	-.025	-----
	4.446	1.104	-----	.000	-.011	-.037	.017	-.023	-----
	4.831	1.113	-----	.005	-.001	-.021	.008	.014	-----
	5.216	1.122	-----	.008	.001	.008	-.015	.022	-----
	5.643	1.132	-----	.018	.013	.028	-.010	.014	-----
	6.028	1.141	-----	.024	.021	.019	.006	.007	-----
	6.455	1.151	-----	.025	.019	.005	.026	.000	-----
	6.840	1.160	-----	.040	.038	.030	.058	.020	-----
	7.652	1.179	-----	-.065	-.066	-.062	-.063	-.034	-----
1,200	0.428	1.010	-----	0.110	0.104	0.119	0.122	0.131	-----
	.812	1.019	-----	.147	.138	.129	.119	.102	-----
	1.197	1.028	-----	.201	.206	.153	.118	.069	-----
	1.625	1.038	-----	.191	.194	.166	.126	.048	-----
	2.009	1.047	-----	.171	.176	.166	.145	.074	-----
	2.437	1.057	-----	.117	.116	.111	.114	.106	-----
	2.822	1.066	-----	.078	.075	.054	.053	.085	-----
	3.206	1.075	-----	.049	.043	.039	.007	.018	-----
	3.634	1.085	-----	.027	.021	.043	-.013	-.026	-----
	4.019	1.094	-----	.008	.002	.011	-.004	-.030	-----
	4.446	1.104	-----	-.007	-.014	-.039	.010	-.031	-----
	4.831	1.113	-----	.000	-.004	-.034	.010	.008	-----
	5.216	1.122	-----	.002	-.002	-.006	-.012	.027	-----
	5.643	1.132	-----	.015	.012	.029	-.017	.020	-----
	6.028	1.141	-----	.022	.019	.029	-.006	.014	-----
	6.455	1.151	-----	.027	.023	.014	.020	.011	-----
	6.840	1.160	-----	.040	.037	.024	.050	.018	-----
	7.652	1.179	-----	-.071	-.069	-.065	-.063	-.042	-----

TABLE I.- FUSELAGE-OVERHANG PRESSURE COEFFICIENTS - Continued

(g) $h/D_j = 0.855$; $\phi = 7^\circ$; $M_\infty = 1.00$

Jet-exit temperature, T_j , $^{\circ}\text{F}$	Orifice location, x'/D_j	Orifice location, x/L	Pressure coefficient for jet pressure ratio H_j/p_0 of -						
			Jet off	2	3	5	7	9	11
80	0.428	1.010	0.183	0.178	0.171	0.160	0.150	-----	-----
	.812	1.019	.200	.197	.198	.164	.130	-----	-----
	1.197	1.028	.216	.235	.238	.189	.168	-----	-----
	1.625	1.038	.214	.225	.231	.226	.223	-----	-----
	2.009	1.047	-----	-----	-----	-----	-----	-----	-----
	2.437	1.057	.185	.173	.181	.186	.198	-----	-----
	2.822	1.066	.153	.132	.138	.126	.124	-----	-----
	3.206	1.075	.127	.102	.106	.107	.090	-----	-----
	3.634	1.085	.100	.077	.076	.117	.075	-----	-----
	4.019	1.094	.071	.047	.048	.081	.088	-----	-----
	4.446	1.104	.044	.019	.015	.011	.066	-----	-----
	4.831	1.113	.034	.006	.000	-.051	.016	-----	-----
	5.216	1.122	.027	.003	.001	-.088	-.042	-----	-----
	5.643	1.132	.035	.013	.009	-.050	-.085	-----	-----
	6.028	1.141	.035	.022	.018	.020	-.088	-----	-----
	6.455	1.151	.040	.034	.035	.057	-.004	-----	-----
	6.840	1.160	.062	.064	.089	.082	-----	-----	-----
	7.652	1.179	.004	.026	.028	.019	.070	-----	-----
800	0.428	1.010	-----	0.187	0.179	0.172	0.156	0.154	0.177
	.812	1.019	-----	.207	.200	.178	.137	.065	.103
	1.197	1.028	-----	.228	.230	.197	.159	.072	-.197
	1.625	1.038	-----	.217	.223	.222	.197	.158	.048
	2.009	1.047	-----	-----	-----	-----	-----	-----	-----
	2.437	1.057	-----	.170	.175	.172	.181	.233	.166
	2.822	1.066	-----	.133	.134	.132	.113	.136	.241
	3.206	1.075	-----	.103	.104	.127	.079	.078	.113
	3.634	1.085	-----	.077	.078	.093	.071	.053	.054
	4.019	1.094	-----	.048	.044	.020	.080	.012	-.004
	4.446	1.104	-----	.023	.015	-.038	.052	.000	.000
	4.831	1.113	-----	.012	.003	-.024	.002	.051	-.042
	5.216	1.122	-----	.007	-.003	.017	-.060	.030	-.030
	5.643	1.132	-----	.015	.010	.028	-.091	-.015	.059
	6.028	1.141	-----	.022	.016	.000	-.073	-.044	.043
	6.455	1.151	-----	.030	.028	-.007	.011	-.045	-.014
	6.840	1.160	-----	.058	.060	.051	.085	.024	.040
	7.652	1.179	-----	.025	.025	.037	.051	.087	.035
1,200	0.428	1.010	-----	0.190	0.180	0.173	0.163	0.170	0.205
	.812	1.019	-----	.206	.196	.182	.136	.051	.200
	1.197	1.028	-----	.227	.229	.197	.156	.042	-.154
	1.625	1.038	-----	.221	.223	.214	.192	.136	-.104
	2.009	1.047	-----	-----	-----	-----	-----	-----	-----
	2.437	1.057	-----	.173	.175	.170	.183	.241	.122
	2.822	1.066	-----	.134	.135	.125	.117	.143	.254
	3.206	1.075	-----	.105	.102	.116	.078	.082	.152
	3.634	1.085	-----	.078	.074	.097	.060	.040	.062
	4.019	1.094	-----	.054	.045	.041	.069	.020	-.012
	4.446	1.104	-----	.024	.011	-.032	.051	-.032	-.018
	4.831	1.113	-----	.013	.002	-.044	.013	.031	-.015
	5.216	1.122	-----	.007	-.005	-.010	-.040	.042	-.045
	5.643	1.132	-----	.017	.007	.027	-.077	-.007	.025
	6.028	1.141	-----	.021	.013	.018	-.077	-.044	.051
	6.455	1.151	-----	.031	.026	.006	-.005	-.034	.003
	6.840	1.160	-----	.059	.058	.044	.076	.018	.033
	7.652	1.179	-----	.027	.025	.040	.058	.074	.037

TABLE I.- FUSELAGE-OVERHANG PRESSURE COEFFICIENTS - Continued

(h) $h/D_j = 0.855$; $\phi = 10^\circ$; $M_\infty = 1.00$

Jet-exit temperature, T_j , °F	Orifice location, x'/D_j	Orifice location, x/L	Pressure coefficient for jet pressure ratio H_j/p_0 of -						
			Jet off	2	3	5	7	9	11
80	0.428	1.010	0.184	0.178	0.166	0.160	0.153	-----	-----
	.812	1.019	.201	.197	.193	.170	.162	-----	-----
	1.197	1.028	-----	-----	-----	-----	-----	-----	-----
	1.625	1.038	.213	.227	.232	.223	.201	-----	-----
	2.009	1.047	-----	-----	-----	-----	-----	-----	-----
	2.437	1.057	.180	.168	.174	.163	.168	-----	-----
	2.822	1.066	.149	.130	.135	.125	.113	-----	-----
	3.206	1.075	.121	.097	.098	.108	.075	-----	-----
	3.634	1.085	.097	.072	.071	.082	.063	-----	-----
	4.019	1.094	.063	.035	.030	.008	.050	-----	-----
	4.446	1.104	.042	.012	.003	-.047	.028	-----	-----
	4.831	1.113	.039	.013	.008	-.038	-.002	-----	-----
	5.216	1.122	.037	.013	.009	.004	-.042	-----	-----
	5.643	1.132	.045	.027	.021	.037	-.060	-----	-----
	6.028	1.141	.051	.042	.040	.040	-.015	-----	-----
	6.455	1.151	.074	.071	.072	.058	.068	-----	-----
	6.840	1.160	.087	.091	.094	.084	.115	-----	-----
	7.652	1.179	.029	.095	.095	.109	.123	-----	-----
800	0.428	1.010	-----	0.183	0.174	0.169	0.161	0.157	0.154
	.812	1.019	-----	.204	.202	.178	.163	.136	.108
	1.197	1.028	-----	-----	-----	-----	-----	-----	-----
	1.625	1.038	-----	.220	.227	.225	.202	.161	.113
	2.009	1.047	-----	-----	-----	-----	-----	-----	-----
	2.437	1.057	-----	.166	.172	.163	.166	.189	.171
	2.822	1.066	-----	.129	.132	.131	.111	.117	.186
	3.206	1.075	-----	.098	.099	.110	.079	.062	.091
	3.634	1.085	-----	.072	.071	.072	.070	.042	.023
	4.019	1.094	-----	.037	.033	.004	.053	.001	.000
	4.446	1.104	-----	.015	.011	-.029	.022	.005	-.029
	4.831	1.113	-----	.015	.009	-.001	-.012	.035	-.033
	5.216	1.122	-----	.015	.009	.020	-.054	.012	.015
	5.643	1.132	-----	.027	.023	.024	-.052	-.014	.051
	6.028	1.141	-----	.042	.039	.023	.009	-.017	.039
	6.455	1.151	-----	.069	.070	.059	.081	.035	.055
	6.840	1.160	-----	.090	.093	.098	.120	.087	.084
	7.652	1.179	-----	.093	.095	.102	.110	.132	.107
1,200	0.428	1.010	-----	0.181	0.176	0.167	0.163	0.160	0.160
	.812	1.019	-----	.198	.190	.174	.160	.131	.115
	1.197	1.028	-----	.214	.219	.189	.154	.088	-.056
	1.625	1.038	-----	.214	.219	.213	.193	.149	.099
	2.009	1.047	-----	-----	-----	-----	-----	-----	-----
	2.437	1.057	-----	.165	.167	.159	.167	.184	.141
	2.822	1.066	-----	.129	.131	.122	.110	.122	.180
	3.206	1.075	-----	.099	.097	.103	.076	.062	.101
	3.634	1.085	-----	.072	.070	.075	.062	.040	.026
	4.019	1.094	-----	.037	.032	.014	.048	.002	-.011
	4.446	1.104	-----	.016	.008	-.028	.022	-.007	-.026
	4.831	1.113	-----	.015	.011	-.013	-.005	.024	-.021
	5.216	1.122	-----	.015	.009	.011	-.045	.010	.007
	5.643	1.132	-----	.025	.022	.028	-.048	-.010	.043
	6.028	1.141	-----	.041	.039	.034	.005	-.003	.041
	6.455	1.151	-----	.065	.066	.057	.074	.040	.055
	6.840	1.160	-----	.085	.087	.088	.113	.083	.083
	7.652	1.179	-----	.088	.091	.103	.109	.123	.104

TABLE I.- FUSELAGE-OVERHANG PRESSURE COEFFICIENTS - Continued

(i) $h/D_j = 1.040; \phi = 7^\circ; M_\infty = 1.00$

Jet-exit temperature, $T_j, {}^{\circ}\text{F}$	Orifice location, x'/D_j	Orifice location, x/L	Pressure coefficient for jet pressure ratio H_j/p_0 of -						
			Jet off	2	3	5	7	9	11
80	0.428	1.010	0.186	0.180	0.170	0.165	0.162	----	----
	.812	1.019	.198	.205	.205	.175	.173	----	----
	1.197	1.028	.210	.235	.237	.222	.189	----	----
	1.625	1.038	.207	.226	.232	.240	.207	----	----
	2.009	1.047	.201	.211	.222	.229	.217	----	----
	2.437	1.057	.179	.172	.181	.180	.183	----	----
	2.822	1.066	.154	.136	.143	.149	.131	----	----
	3.206	1.075	.127	.103	.107	.127	.095	----	----
	3.634	1.085	.101	.075	.077	.084	.084	----	----
	4.019	1.094	.075	.048	.046	.017	.081	----	----
	4.446	1.104	.053	.025	.018	-.028	.050	----	----
	4.831	1.113	.041	.015	.008	-.001	.012	----	----
	5.216	1.122	.035	.009	-.001	.022	-.053	----	----
	5.643	1.132	.042	.022	.015	.025	-.088	----	----
	6.028	1.141	.051	.039	.035	.008	-.052	----	----
	6.455	1.151	.057	.050	.048	.014	.027	----	----
	6.840	1.160	.072	.075	.077	.073	.097	----	----
	7.652	1.179	-.025	-.025	-.026	-.018	-.006	----	----
800	0.428	1.010	----	0.183	0.173	0.176	0.167	0.164	0.167
	.812	1.019	----	.200	.197	.175	.170	.153	.144
	1.197	1.028	----	.226	.228	.203	.178	.151	.111
	1.625	1.038	----	.220	.223	.222	.190	.158	.080
	2.009	1.047	----	.208	.212	.216	.198	.179	.084
	2.437	1.057	----	.170	.173	.174	.172	.174	.124
	2.822	1.066	----	.135	.137	.141	.126	.129	.172
	3.206	1.075	----	.103	.104	.119	.087	.076	.123
	3.634	1.085	----	.075	.074	.083	.065	.040	.049
	4.019	1.094	----	.048	.045	.025	.061	.014	-.006
	4.446	1.104	----	.024	.018	-.020	.048	.012	-.020
	4.831	1.113	----	.014	.006	-.007	.019	.032	-.037
	5.216	1.122	----	.008	.000	.015	-.028	.009	-.042
	5.643	1.132	----	.021	.014	.023	-.060	-.010	.035
	6.028	1.141	----	.036	.032	.014	-.052	-.015	.060
	6.455	1.151	----	.046	.045	.020	.011	-.007	.052
	6.840	1.160	----	.071	.071	.070	.080	.044	.055
	7.652	1.179	----	-.020	-.021	-.014	.012	.018	-.015
1,200	0.428	1.010	----	0.180	0.173	0.176	0.175	0.173	0.179
	.812	1.019	----	.195	.189	.179	.175	.157	.153
	1.197	1.028	----	.223	.225	.198	.183	.146	.117
	1.625	1.038	----	.219	.222	.215	.195	.149	.087
	2.009	1.047	----	.207	.213	.214	.205	.171	.085
	2.437	1.057	----	.171	.176	.174	.175	.178	.121
	2.822	1.066	----	.135	.139	.138	.124	.139	.172
	3.206	1.075	----	.103	.106	.118	.084	.078	.125
	3.634	1.085	----	.074	.074	.090	.069	.039	.052
	4.019	1.094	----	.047	.045	.030	.069	.012	-.008
	4.446	1.104	----	.021	.015	-.027	.046	.000	-.021
	4.831	1.113	----	.014	.007	-.025	.012	.032	-.032
	5.216	1.122	----	.007	.000	.003	-.044	.015	-.036
	5.643	1.132	----	.017	.013	.028	-.081	-.012	.036
	6.028	1.141	----	.036	.034	.025	-.049	-.007	.048
	6.455	1.151	----	.048	.050	.027	.033	.005	.032
	6.840	1.160	----	.069	.072	.062	.092	.038	.056
	7.652	1.179	----	-.024	-.023	-.015	-.008	.011	-.016

TABLE I. - FUSELAGE-OVERHANG PRESSURE COEFFICIENTS - Continued

(j) $h/D_j = 0.855$; $\phi = 7^\circ$; $M_\infty = 1.10$

Jet-exit temperature, $T_j, {}^{\circ}\text{F}$	Orifice location, x'/D_j	Orifice location, x/L	Pressure coefficient for jet pressure ratio H_j/p_0 of -						
			Jet off	2	3	5	7	9	11
80	0.428	1.010	0.113	0.143	0.134	0.141	0.126	-----	-----
	.812	1.019	.129	.167	.155	.148	.101	-----	-----
	1.197	1.028	.150	.198	.203	.167	.128	-----	-----
	1.625	1.038	.160	.195	.207	.198	.178	-----	-----
	2.009	1.047	-----	-----	-----	-----	-----	-----	-----
	2.437	1.057	.146	.153	.164	.164	.189	-----	-----
	2.822	1.066	.119	.111	.126	.101	.117	-----	-----
	3.206	1.075	.095	.081	.087	.105	.069	-----	-----
	3.634	1.085	.068	.054	.055	.103	.014	-----	-----
	4.019	1.094	.041	.023	.036	.058	.002	-----	-----
	4.446	1.104	.010	-.004	.001	-.003	.040	-----	-----
	4.831	1.113	-.007	-.021	-.034	-.056	.009	-----	-----
	5.216	1.122	-.027	-.038	-.044	-.072	-.029	-----	-----
	5.643	1.132	-.041	-.050	-.040	-.056	-.048	-----	-----
	6.028	1.141	-.071	-.079	-.075	-.075	-.094	-----	-----
	6.455	1.151	-.094	-.107	-.117	-.105	-.142	-----	-----
	6.840	1.160	-.085	-.085	-.084	-.066	-.086	-----	-----
	7.652	1.179	-.189	-.196	-.256	-.307	-.310	-----	-----
800	0.428	1.010	-----	0.150	0.143	0.140	0.133	0.130	0.152
	.812	1.019	-----	.161	.155	.148	.114	.044	.094
	1.197	1.028	-----	.186	.190	.163	.135	.028	-.115
	1.625	1.038	-----	.186	.194	.195	.173	.092	.019
	2.009	1.047	-----	-----	-----	-----	-----	-----	-----
	2.437	1.057	-----	.152	.159	.155	.171	.202	-.002
	2.822	1.066	-----	.113	.121	.117	.104	.150	.131
	3.206	1.075	-----	.083	.092	.121	.059	.087	.155
	3.634	1.085	-----	.057	.065	.092	.027	.054	.130
	4.019	1.094	-----	.026	.030	.023	.040	.011	.073
	4.446	1.104	-----	-.003	.002	-.043	.034	-.061	.026
	4.831	1.113	-----	-.018	-.014	-.066	.003	-.071	-.003
	5.216	1.122	-----	-.039	-.039	-.038	-.050	-.006	-.073
	5.643	1.132	-----	-.053	-.049	-.031	-.059	.003	-.095
	6.028	1.141	-----	-.079	-.077	-.059	-.105	-.072	-.115
	6.455	1.151	-----	-.105	-.107	-.104	-.141	-.131	-.139
	6.840	1.160	-----	-.090	-.088	-.094	-.086	-.081	-.060
	7.652	1.179	-----	-.184	-.214	-.274	-.297	-.317	-.317
1,200	0.428	1.010	-----	0.143	0.131	0.132	0.128	0.141	0.164
	.812	1.019	-----	.153	.138	.138	.103	.051	.117
	1.197	1.028	-----	.179	.177	.155	.110	.005	-.133
	1.625	1.038	-----	.180	.185	.174	.145	.053	-.023
	2.009	1.047	-----	-----	-----	-----	-----	-----	-----
	2.437	1.057	-----	.141	.146	.143	.160	.148	-.035
	2.822	1.066	-----	.103	.106	.095	.100	.156	.010
	3.206	1.075	-----	.075	.080	.093	.057	.105	.156
	3.634	1.085	-----	.049	.047	.085	.011	.049	.116
	4.019	1.094	-----	.019	.019	.037	-.006	.024	.100
	4.446	1.104	-----	-.013	-.011	-.034	.009	-.052	.018
	4.831	1.113	-----	-.026	-.029	-.067	-.003	-.089	-.006
	5.216	1.122	-----	-.044	-.050	-.072	-.034	-.084	-.054
	5.643	1.132	-----	-.056	-.056	-.054	-.052	-.020	-.086
	6.028	1.141	-----	-.084	-.084	-.072	-.100	-.047	-.117
	6.455	1.151	-----	-.109	-.115	-.102	-.150	-.123	-.153
	6.840	1.160	-----	-.095	-.094	-.085	-.096	-.089	-.100
	7.652	1.179	-----	-.174	-.206	-.254	-.292	-.312	-.302

TABLE I.- FUSELAGE-OVERHANG PRESSURE COEFFICIENTS - Continued

(k) $h/D_j = 0.855$; $\phi = 10^\circ$; $M_\infty = 1.10$

Jet-exit temperature, T_j , °F	Orifice location, x'/D_j	Orifice location, x/L	Pressure coefficient for jet pressure ratio H_j/p_0 of -					
			Jet off	2	3	5	7	9
80	0.428	1.010	0.126	0.137	0.123	0.128	0.125	-----
	.812	1.019	.143	.148	.134	.138	.128	-----
	1.197	1.028	-----	-----	-----	-----	-----	-----
	1.625	1.038	.171	.194	.201	.183	.165	-----
	2.009	1.047	-----	-----	-----	-----	-----	-----
	2.437	1.057	.148	.143	.152	.139	.148	-----
	2.822	1.066	.123	.103	.109	.093	.096	-----
	3.206	1.075	.096	.070	.073	.086	.047	-----
	3.634	1.085	.071	.044	.049	.080	.006	-----
	4.019	1.094	.035	.004	.001	.029	-.014	-----
	4.446	1.104	.007	-.022	-.029	-.027	-.004	-----
	4.831	1.113	-.004	-.027	-.023	-.056	-.007	-----
	5.216	1.122	-.021	-.042	-.041	-.071	-.035	-----
	5.643	1.132	-.039	-.057	-.063	-.071	-.059	-----
	6.028	1.141	-.068	-.084	-.088	-.086	-.099	-----
	6.455	1.151	-.074	-.091	-.091	-.084	-.116	-----
	6.840	1.160	-.069	-.083	-.085	-.079	-.096	-----
	7.652	1.179	-.057	-.074	-.087	-.103	-.112	-----
800	0.428	1.010	-----	0.146	0.138	0.134	0.132	0.136
	.812	1.019	-----	.158	.153	.146	.137	.114
	1.197	1.028	-----	-----	-----	-----	-----	-----
	1.625	1.038	-----	.184	.194	.188	.171	.114
	2.009	1.047	-----	-----	-----	-----	-----	0.079
	2.437	1.057	-----	.139	.151	.144	.146	.168
	2.822	1.066	-----	.103	.114	.115	.092	.119
	3.206	1.075	-----	.071	.081	.103	.047	.057
	3.634	1.085	-----	.045	.053	.070	.018	.036
	4.019	1.094	-----	.007	.012	.001	.013	-.026
	4.446	1.104	-----	-.018	-.015	-.054	.005	-.078
	4.831	1.113	-----	-.025	-.020	-.056	-.006	-.052
	5.216	1.122	-----	-.042	-.038	-.046	-.036	-.014
	5.643	1.132	-----	-.059	-.056	-.046	-.068	-.028
	6.028	1.141	-----	-.085	-.084	-.070	-.124	-.082
	6.455	1.151	-----	-.091	-.092	-.091	-.113	-.103
	6.840	1.160	-----	-.083	-.085	-.097	-.097	-.092
	7.652	1.179	-----	-.067	-.081	-.097	-.103	-.122
1,200	0.428	1.010	-----	0.146	0.137	0.135	0.134	0.143
	.812	1.019	-----	.158	.149	.146	.133	.118
	1.197	1.028	-----	-----	-----	-----	-----	-----
	1.625	1.038	-----	.187	.190	.181	.164	.104
	2.009	1.047	-----	-----	-----	-----	-----	0.075
	2.437	1.057	-----	.146	.154	.140	.151	.157
	2.822	1.066	-----	.110	.115	.102	.093	.130
	3.206	1.075	-----	.078	.081	.090	.048	.065
	3.634	1.085	-----	.052	.056	.075	.009	.032
	4.019	1.094	-----	.014	.012	.017	-.009	-.012
	4.446	1.104	-----	-.015	-.017	-.037	-.002	-.064
	4.831	1.113	-----	-.021	-.021	-.055	-.005	-.069
	5.216	1.122	-----	-.038	-.039	-.064	-.032	-.044
	5.643	1.132	-----	-.056	-.056	-.060	-.059	-.029
	6.028	1.141	-----	-.082	-.086	-.080	-.107	-.076
	6.455	1.151	-----	-.086	-.092	-.083	-.120	-.102
	6.840	1.160	-----	-.078	-.084	-.086	-.101	-.094
	7.652	1.179	-----	-.060	-.079	-.093	-.105	-.113

TABLE I.- FUSELAGE-OVERHANG PRESSURE COEFFICIENTS - Concluded

(1) $h/D_j = 1.040$; $\phi = 7^\circ$; $M_\infty = 1.10$

Jet-exit temperature, T_j , °F	Orifice location, x'/D_j	Orifice location, x/L	Pressure coefficient for jet pressure ratio H_j/p_0 of						
			Jet off	2	3	5	7	9	11
80	0.428	1.010	0.121	0.134	0.118	0.125	0.122	-----	-----
	.812	1.019	.137	.151	.142	.121	.131	-----	-----
	1.197	1.028	.153	.191	.193	.154	.147	-----	-----
	1.625	1.038	.158	.193	.202	.196	.163	-----	-----
	2.009	1.047	.159	.186	.199	.212	.180	-----	-----
	2.437	1.057	.146	.151	.165	.167	.165	-----	-----
	2.822	1.066	.126	.114	.126	.124	.120	-----	-----
	3.206	1.075	.101	.080	.091	.118	.065	-----	-----
	3.634	1.085	.076	.052	.059	.096	.019	-----	-----
	4.019	1.094	.048	.023	.026	.042	.024	-----	-----
	4.446	1.104	.023	-.003	.003	-.026	.021	-----	-----
	4.831	1.113	.004	-.018	-.016	-.064	-.001	-----	-----
	5.216	1.122	-.018	-.037	-.043	-.061	-.028	-----	-----
	5.643	1.132	-.034	-.049	-.047	-.046	-.052	-----	-----
	6.028	1.141	-.054	-.067	-.063	-.054	-.086	-----	-----
	6.455	1.151	-.080	-.093	-.103	-.091	-.140	-----	-----
	6.840	1.160	-.074	-.079	-.081	-.080	-.089	-----	-----
	7.652	1.179	-.270	-.331	-.365	-.375	-.378	-----	-----
800	0.428	1.010	-----	0.140	0.131	0.132	0.129	0.144	0.147
	.812	1.019	-----	.154	.147	.135	.137	.126	.130
	1.197	1.028	-----	.180	.183	.157	.148	.094	.099
	1.625	1.038	-----	.179	.186	.188	.161	.059	.060
	2.009	1.047	-----	.171	.182	.199	.175	.056	.022
	2.437	1.057	-----	.139	.153	.164	.156	.032	-.019
	2.822	1.066	-----	.106	.120	.137	.112	.111	.063
	3.206	1.075	-----	.074	.088	.119	.061	.126	.122
	3.634	1.085	-----	.047	.059	.076	.024	.099	.115
	4.019	1.094	-----	.019	.029	.014	.029	.051	.080
	4.446	1.104	-----	-.006	.000	-.045	.022	.010	.026
	4.831	1.113	-----	-.022	-.017	-.045	.001	-.030	.000
	5.216	1.122	-----	-.041	-.038	-.033	-.032	-.082	-.056
	5.643	1.132	-----	-.055	-.052	-.032	-.061	-.099	-.092
	6.028	1.141	-----	-.072	-.070	-.053	-.095	-.103	-.106
	6.455	1.151	-----	-.097	-.098	-.106	-.133	-.115	-.100
	6.840	1.160	-----	-.086	-.083	-.099	-.096	-.069	-.105
	7.652	1.179	-----	-.245	-.340	-.366	-.372	-.361	-.337
1,200	0.428	1.010	-----	0.147	0.149	0.138	0.137	0.140	0.153
	.812	1.019	-----	.156	.185	.145	.141	.127	.139
	1.197	1.028	-----	.184	.195	.158	.151	.108	.109
	1.625	1.038	-----	.193	.193	.181	.164	.094	.070
	2.009	1.047	-----	.186	.162	.196	.178	.113	.032
	2.437	1.057	-----	.154	.128	.166	.165	.145	-.023
	2.822	1.066	-----	.121	.097	.135	.123	.144	.050
	3.206	1.075	-----	.089	.066	.121	.075	.096	.124
	3.634	1.085	-----	.062	.066	.094	.031	.044	.122
	4.019	1.094	-----	.031	.035	.035	.022	.009	.084
	4.446	1.104	-----	.003	.003	-.031	.021	-.052	.020
	4.831	1.113	-----	-.014	-.012	-.053	.005	-.073	-.011
	5.216	1.122	-----	-.032	-.032	-.050	-.028	-.049	-.059
	5.643	1.132	-----	-.049	-.046	-.040	-.052	-.013	-.092
	6.028	1.141	-----	-.066	-.065	-.053	-.083	-.055	-.107
	6.455	1.151	-----	-.092	-.094	-.092	-.123	-.114	-.131
	6.840	1.160	-----	-.081	-.081	-.088	-.094	-.090	-.097
	7.652	1.179	-----	-.282	-.342	-.365	-.370	-.366	-.352

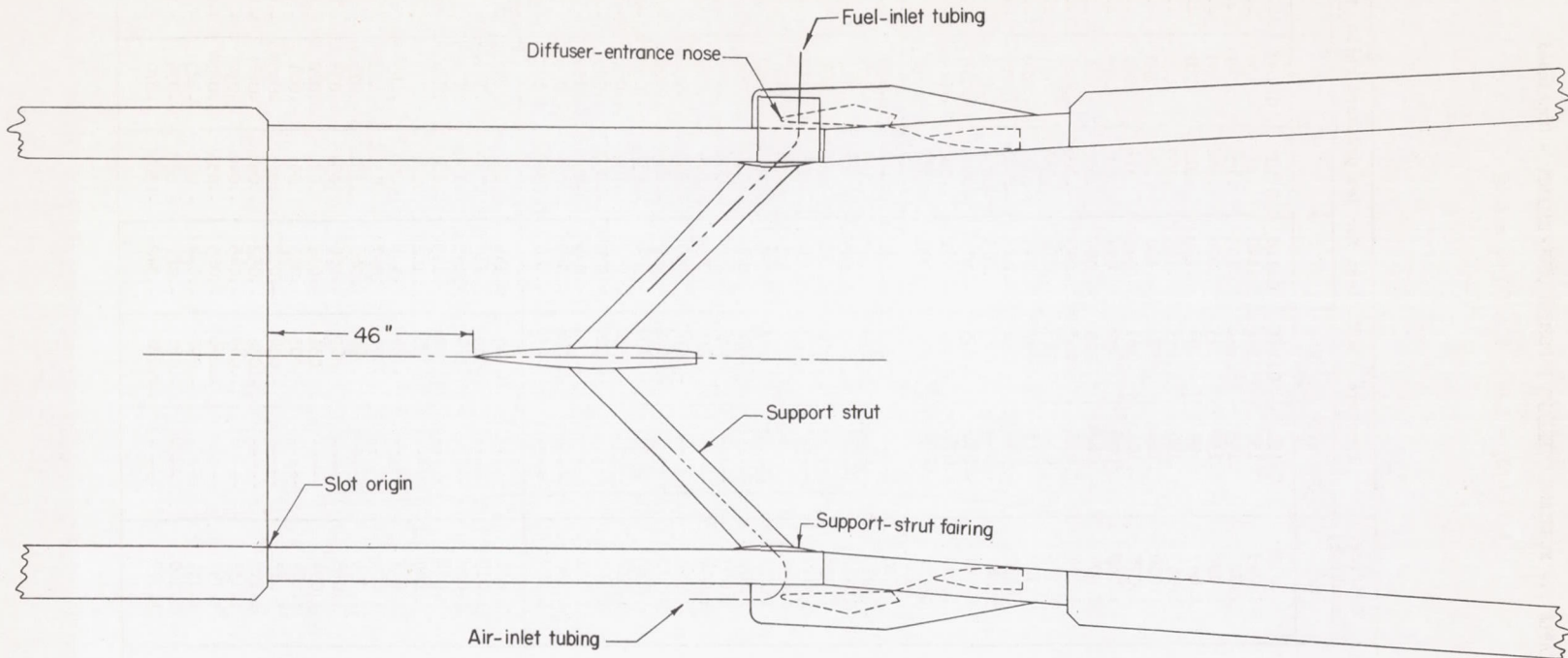


Figure 1.- Side view of basic-fuselage model in Langley 8-foot transonic tunnel.

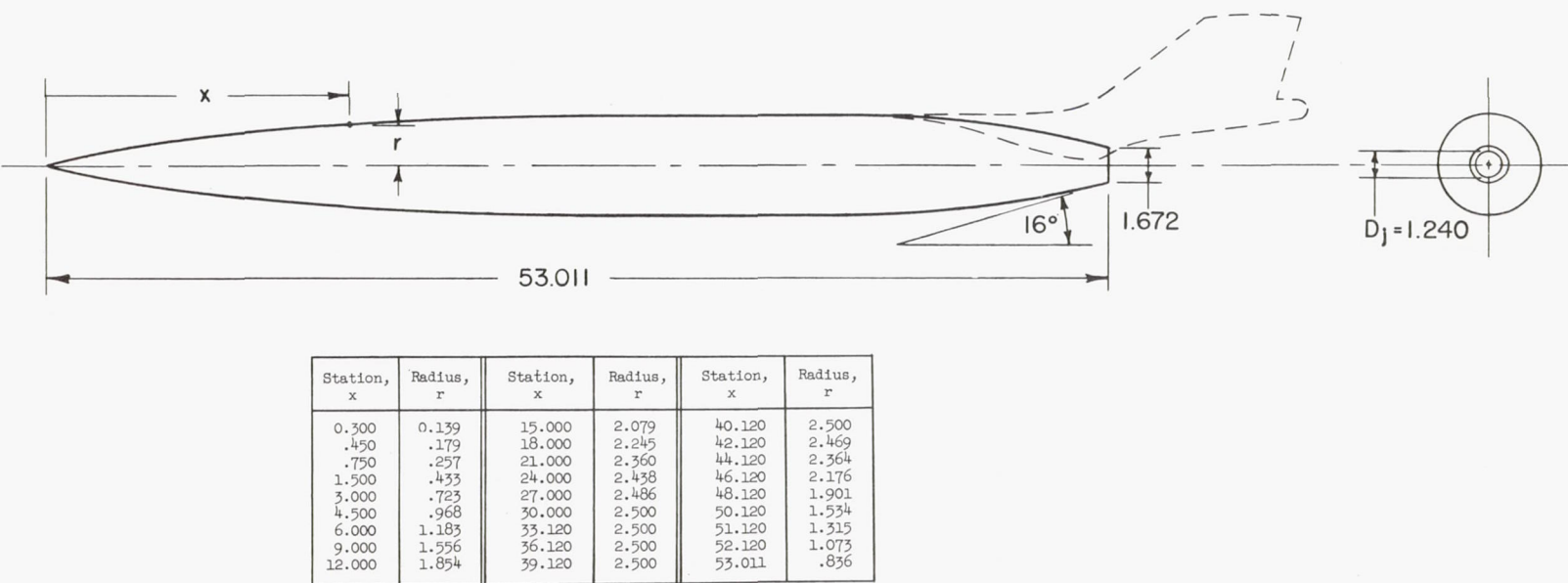
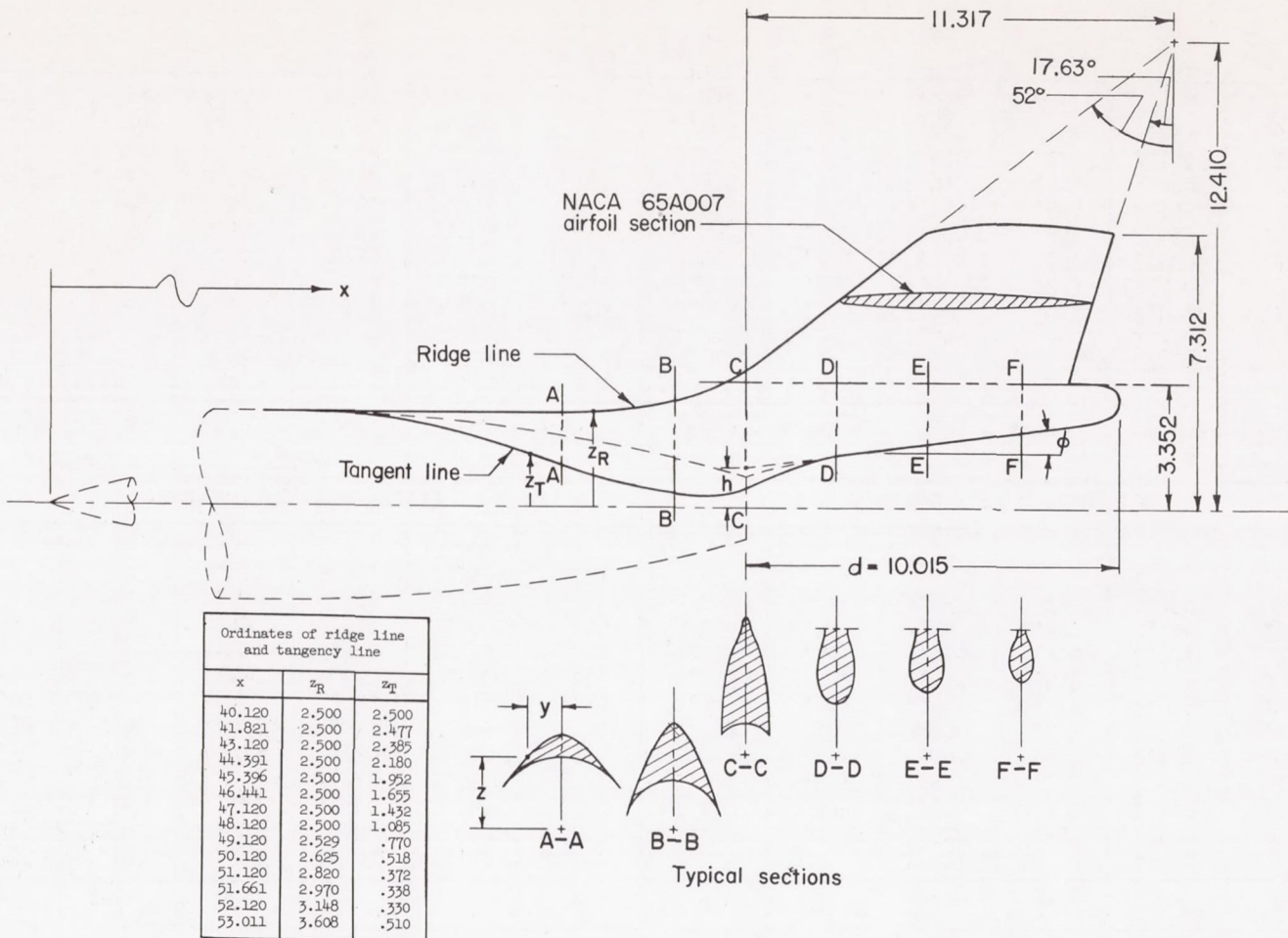


Figure 2.- Ordinates of basic body of revolution. All linear dimensions are in inches.



(a) Sketch of fuselage overhang and vertical tail.

Figure 3.- Details of geometry of fuselage overhangs. All linear dimensions are in inches.

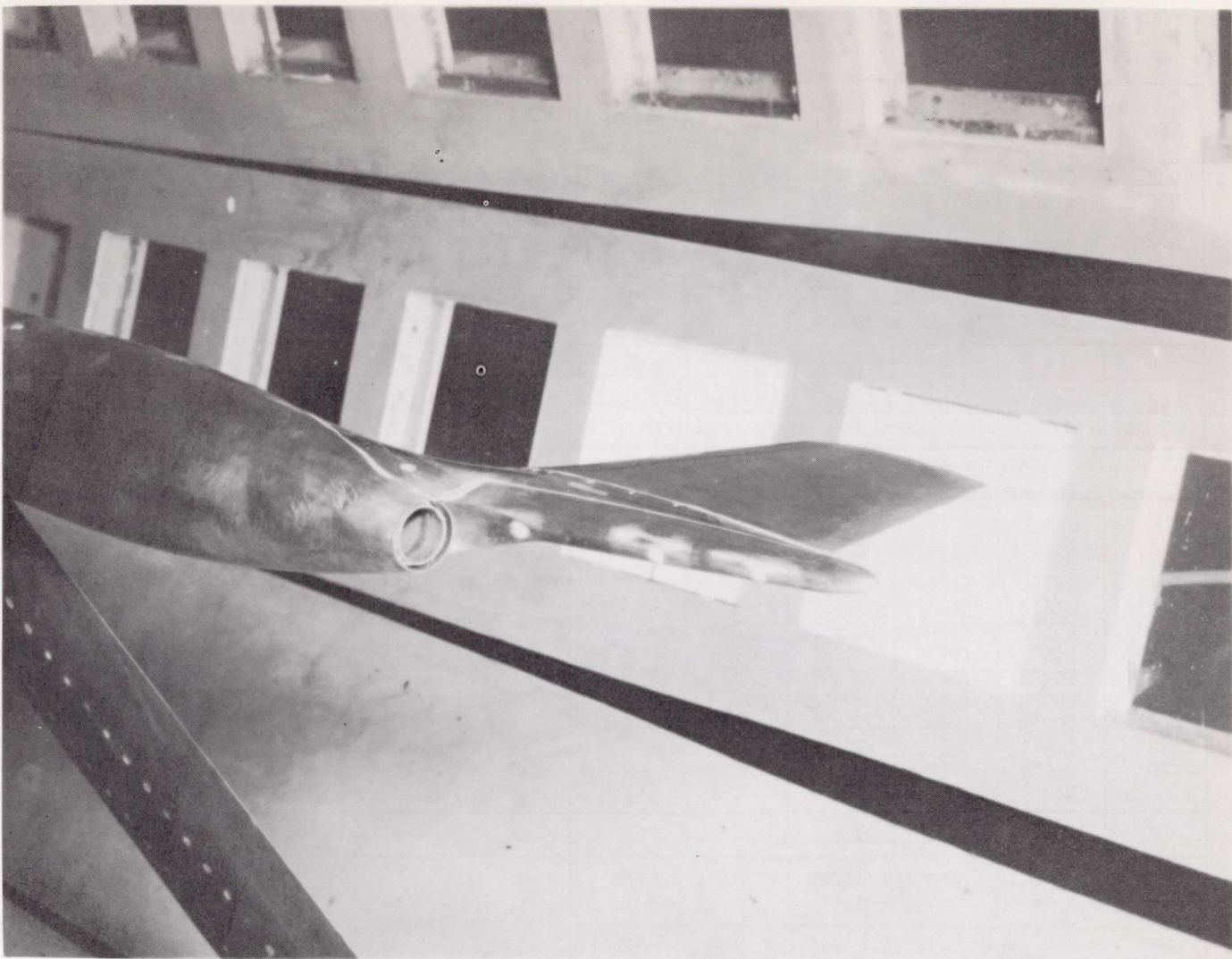
Section A-A x = 48.120		Section B-B x = 51.120		Section C-C x = 53.011		Section D-D; x = 55.429							
z	y	z	y	z	y	$\phi = 7^\circ$ $h/D_j = 0.855$		$\phi = 7^\circ$ $h/D_j = 1.040$		$\phi = 10^\circ$ $h/D_j = 0.855$			
						z	y	z	y	z	y	z	y
1.085	1.561	0.372	1.261	0.510	0.662	1.345	0	1.581	0	1.486	0		
1.345	1.380	.600	1.184	1.000	.618	1.400	.192	1.600	.131	1.500	.073		
1.599	1.180	.833	1.106	1.345	.600	1.600	.383	1.700	.300	1.600	.252		
1.840	.965	1.100	1.012	1.583	.582	1.800	.461	1.800	.384	1.800	.399		
2.050	.748	1.345	.920	1.840	.562	2.000	.495	2.000	.467	2.000	.469		
2.270	.480	1.600	.817	2.066	.534	2.200	.500	2.200	.497	2.200	.497		
2.500	0	1.840	.712	2.270	.500	2.500	.487	2.500	.487	2.500	.487		
		2.050	.614	2.500	.446	2.755	.442	2.755	.442	2.755	.442		
		2.270	.500	2.755	.370	2.916	.385	2.916	.385	2.916	.385		
		2.500	.361	3.000	.255	3.166	.323	3.166	.323	3.166	.323		
		2.700	.195	3.166	.188	3.352	.292	3.352	.292	3.352	.292		
		2.820	0	3.352	.131	3.608	0						
Section E-E; x = 57.833						Section F-F; x = 60.359							
$\phi = 7^\circ$ $h/D_j = 0.855$		$\phi = 7^\circ$ $h/D_j = 1.040$		$\phi = 10^\circ$ $h/D_j = 0.855$		$\phi = 7^\circ$ $h/D_j = 0.855$		$\phi = 7^\circ$ $h/D_j = 1.040$		$\phi = 10^\circ$ $h/D_j = 0.855$			
z	y	z	y	z	y	z	y	z	y	z	y	z	y
1.650	0	1.878	0	1.916	0	1.970	0	2.189	0	2.356	0		
1.700	.165	1.900	.120	2.000	.240	2.000	.103	2.200	.061	2.400	.151		
1.900	.348	2.000	.273	2.100	.342	2.200	.284	2.300	.233	2.500	.263		
2.100	.423	2.100	.359	2.300	.437	2.400	.353	2.400	.307	2.600	.314		
2.300	.458	2.300	.443	2.500	.459	2.600	.364	2.600	.359	2.655	.336		
2.500	.461	2.500	.461	2.755	.418	2.755	.350	2.755	.350	2.916	.304		
2.755	.418	2.755	.418	2.916	.362	2.916	.304	2.916	.304	3.070	.228		
2.916	.362	2.916	.362	3.166	.274	3.070	.228	3.070	.228	3.166	.158		
3.166	.274	3.166	.274	3.352	.272	3.166	.158	3.166	.158	3.352	.093		
3.352	.272	3.352	.272			3.352	.093	3.352	.093				

(b) Coordinates of typical cross sections.

Figure 3.- Concluded.

NACA RM L56A27

27



L-85498

Figure 4.- Three-quarter view of jet exit and fuselage overhang of model mounted in Langley 8-foot transonic tunnel.

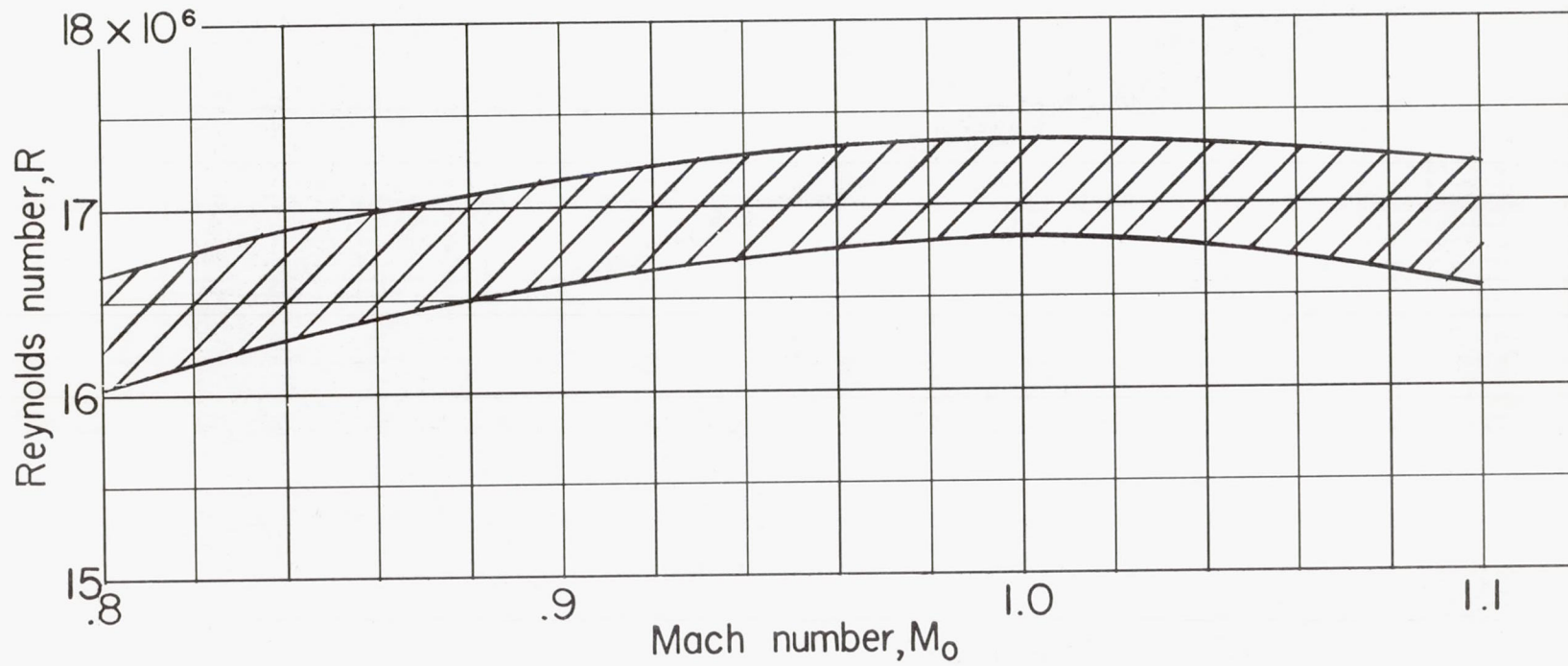


Figure 5.- Variation of Reynolds number based on body length ($L = 53.011$ in.) with Mach number.

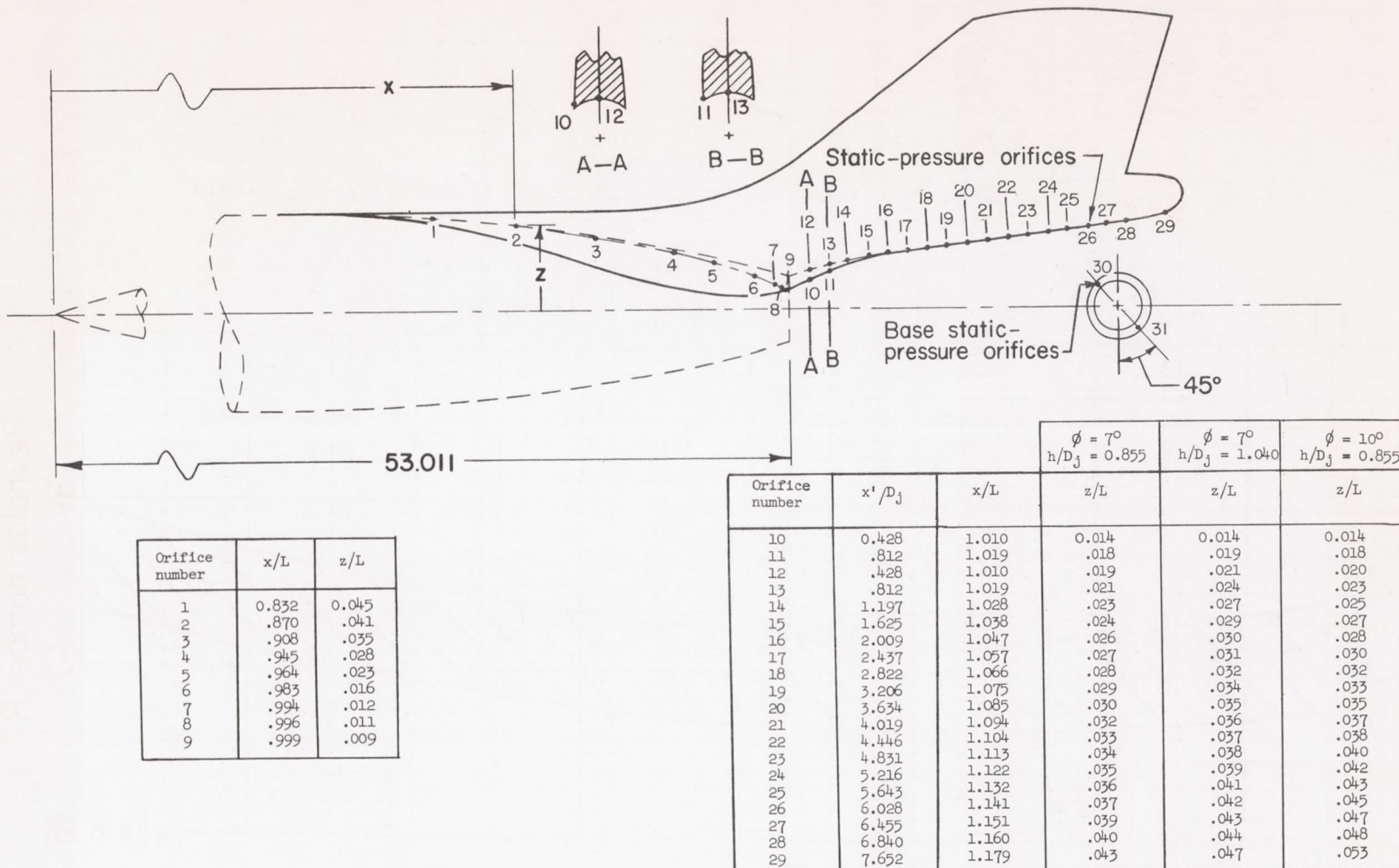


Figure 6.- Location of static-pressure orifices. All linear dimensions are in inches.

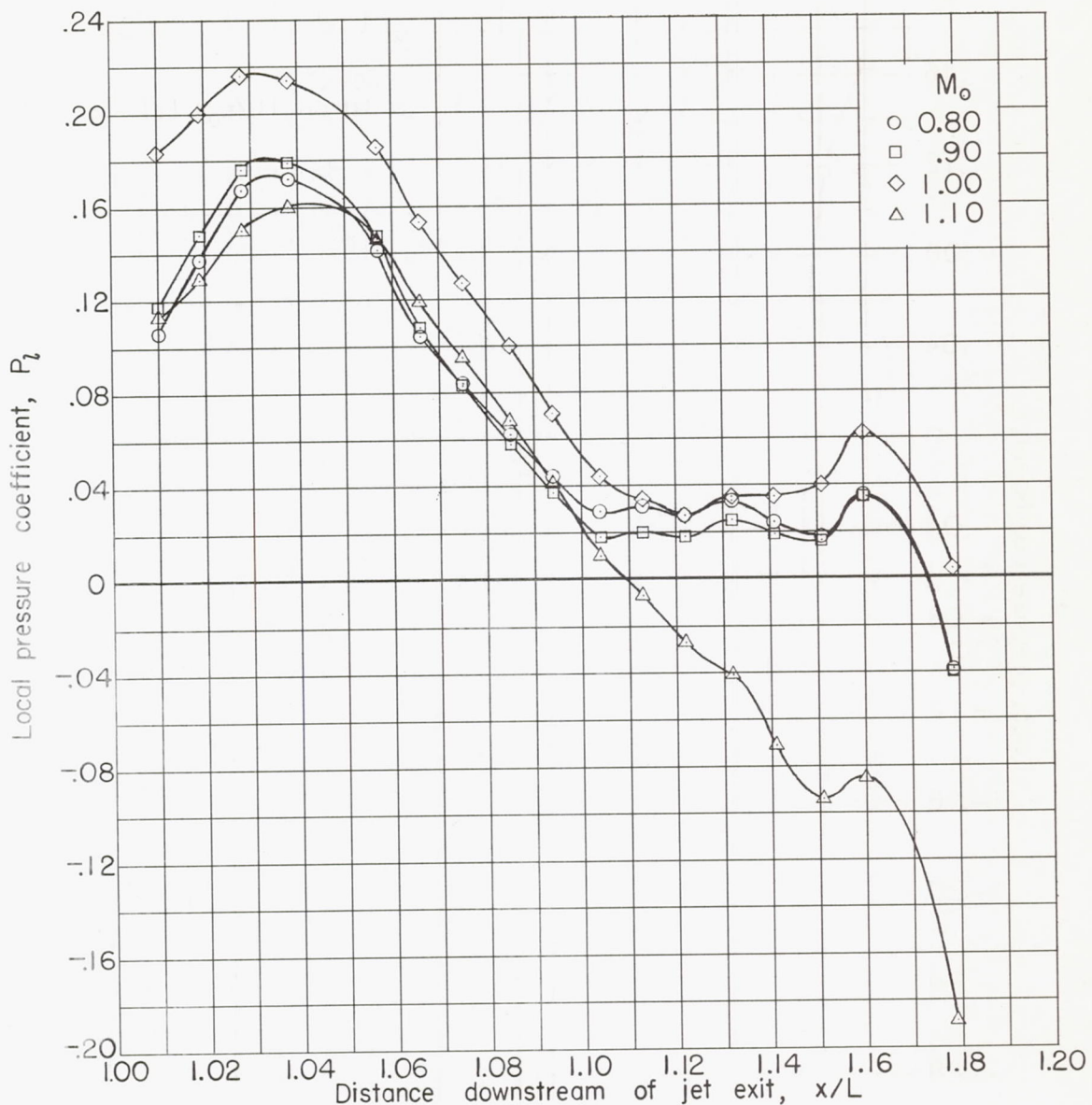


Figure 7.- Typical pressure distributions along fuselage overhang with jet off. $\phi = 7^\circ$; $h/D_j = 0.855$.

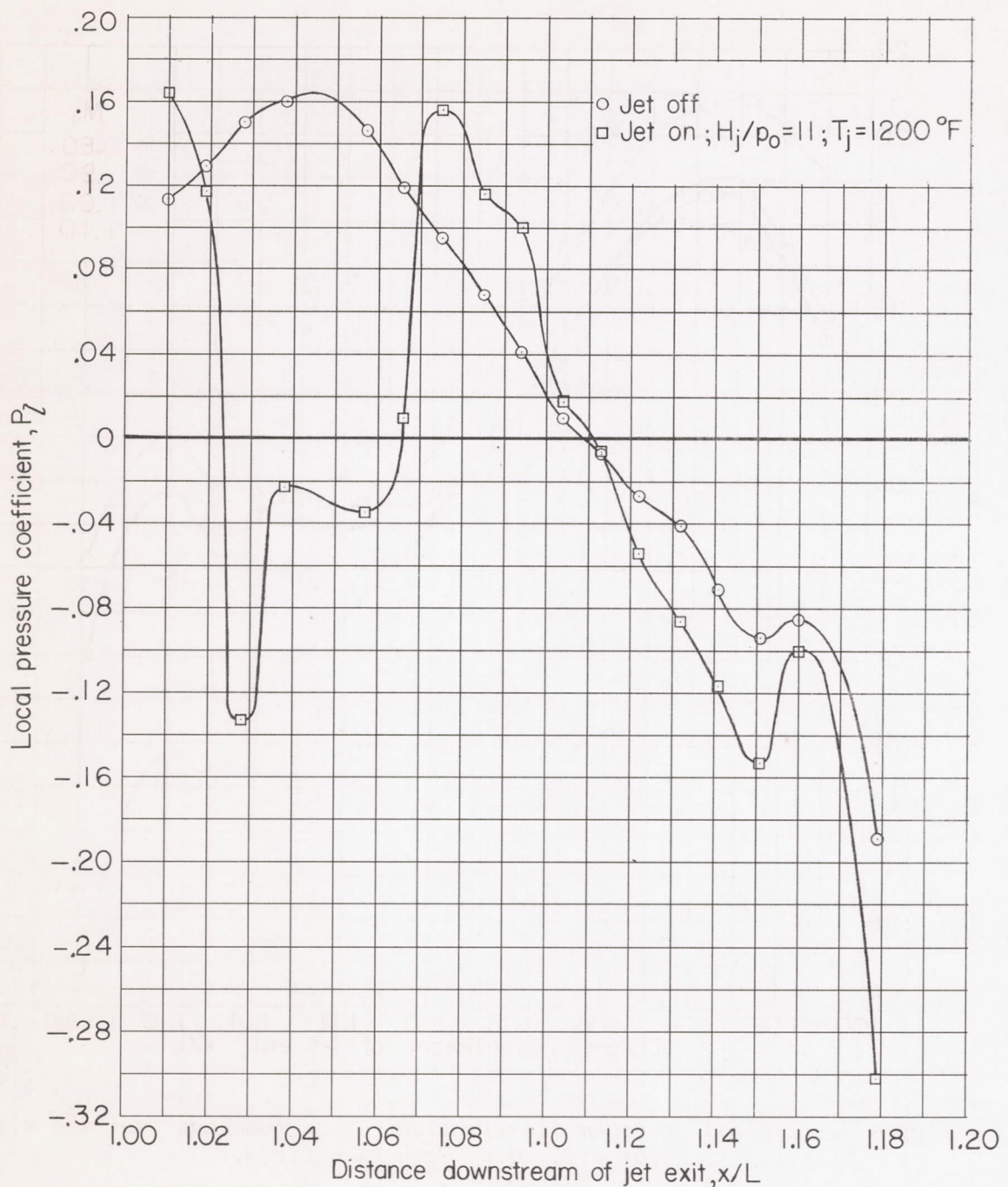
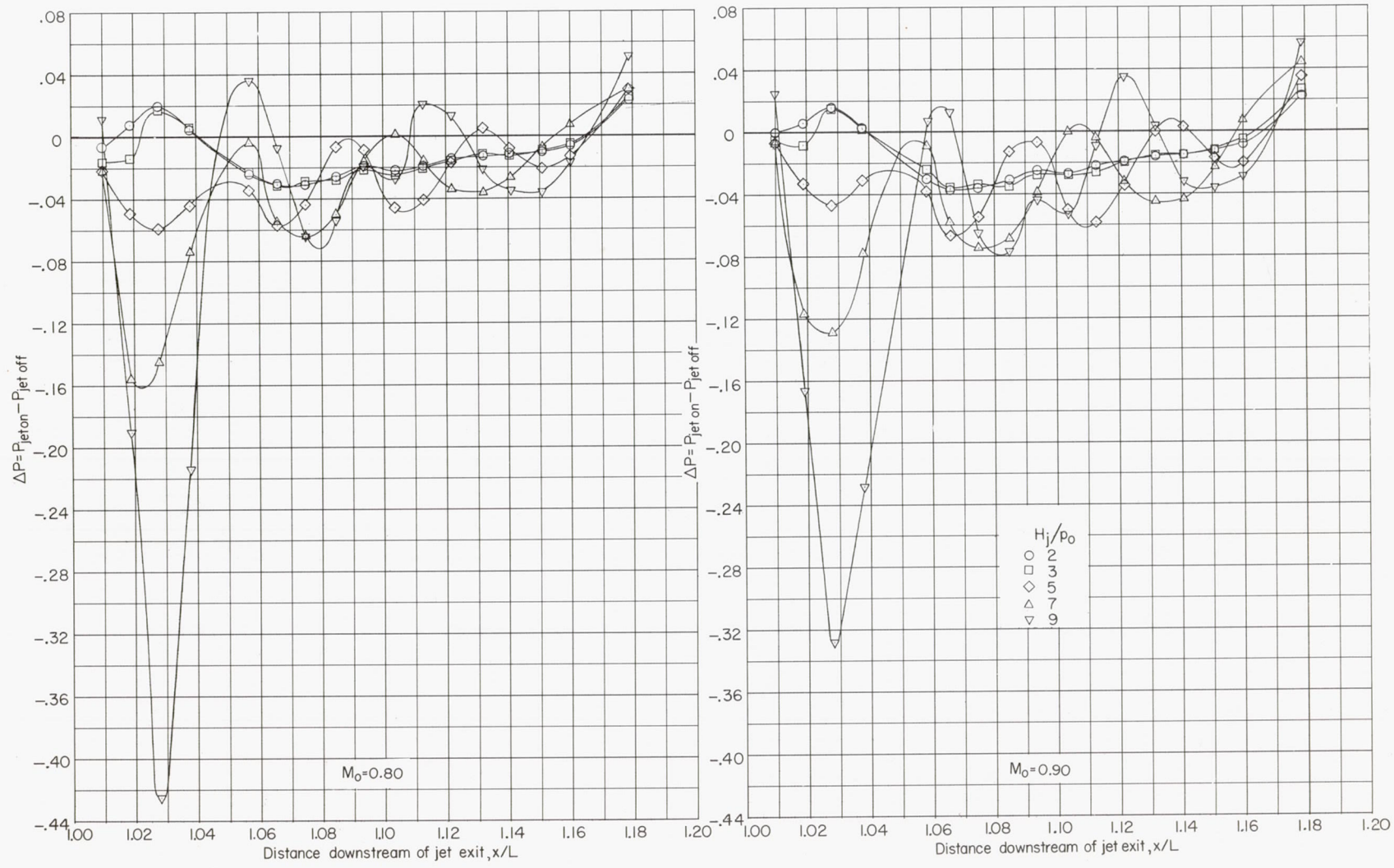
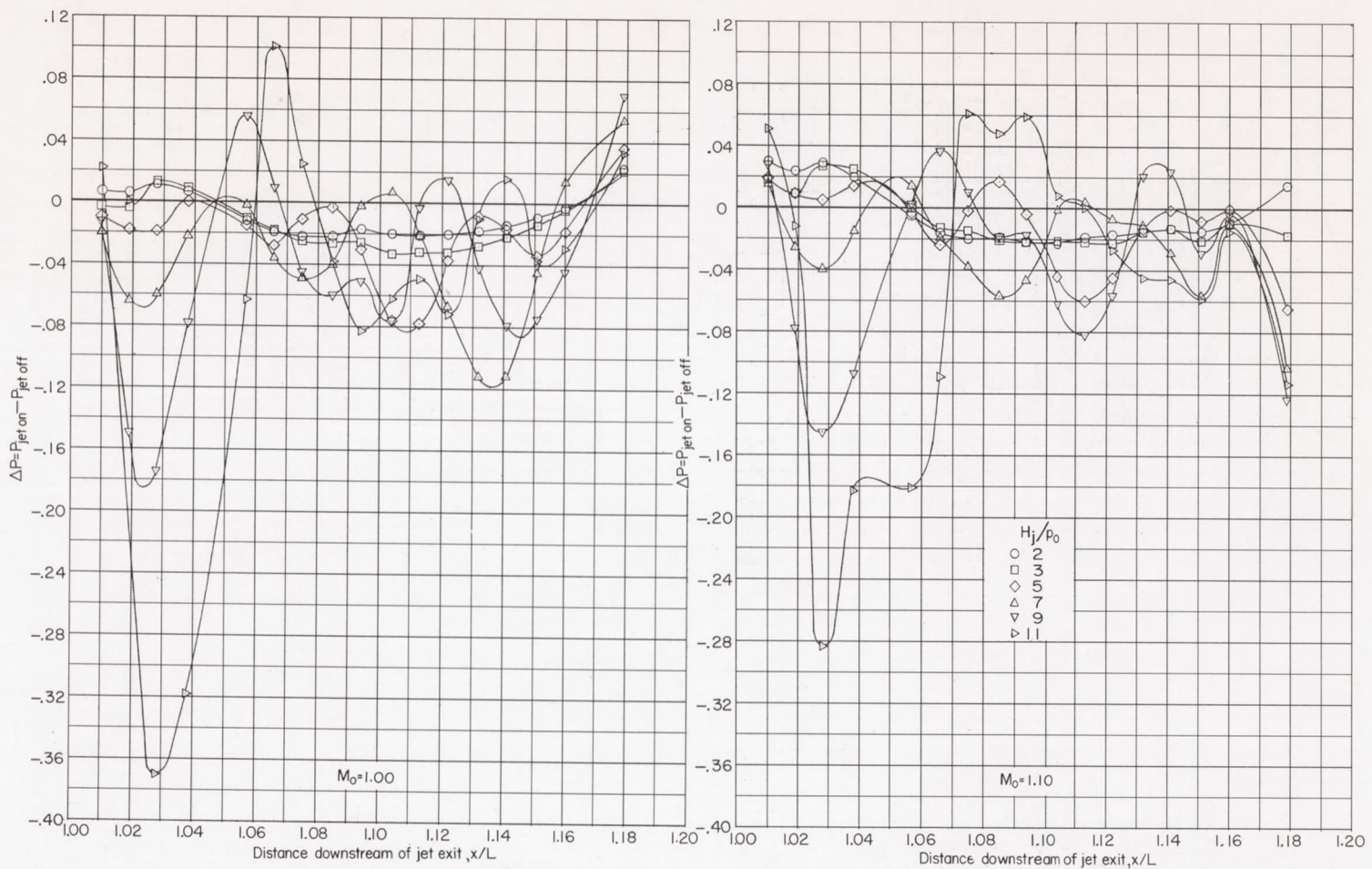


Figure 8.- Comparison of pressure distribution along fuselage overhang with jet on and jet off. $\phi = 7^\circ$; $h/D_j = 0.855$; $M_\infty = 1.10$.



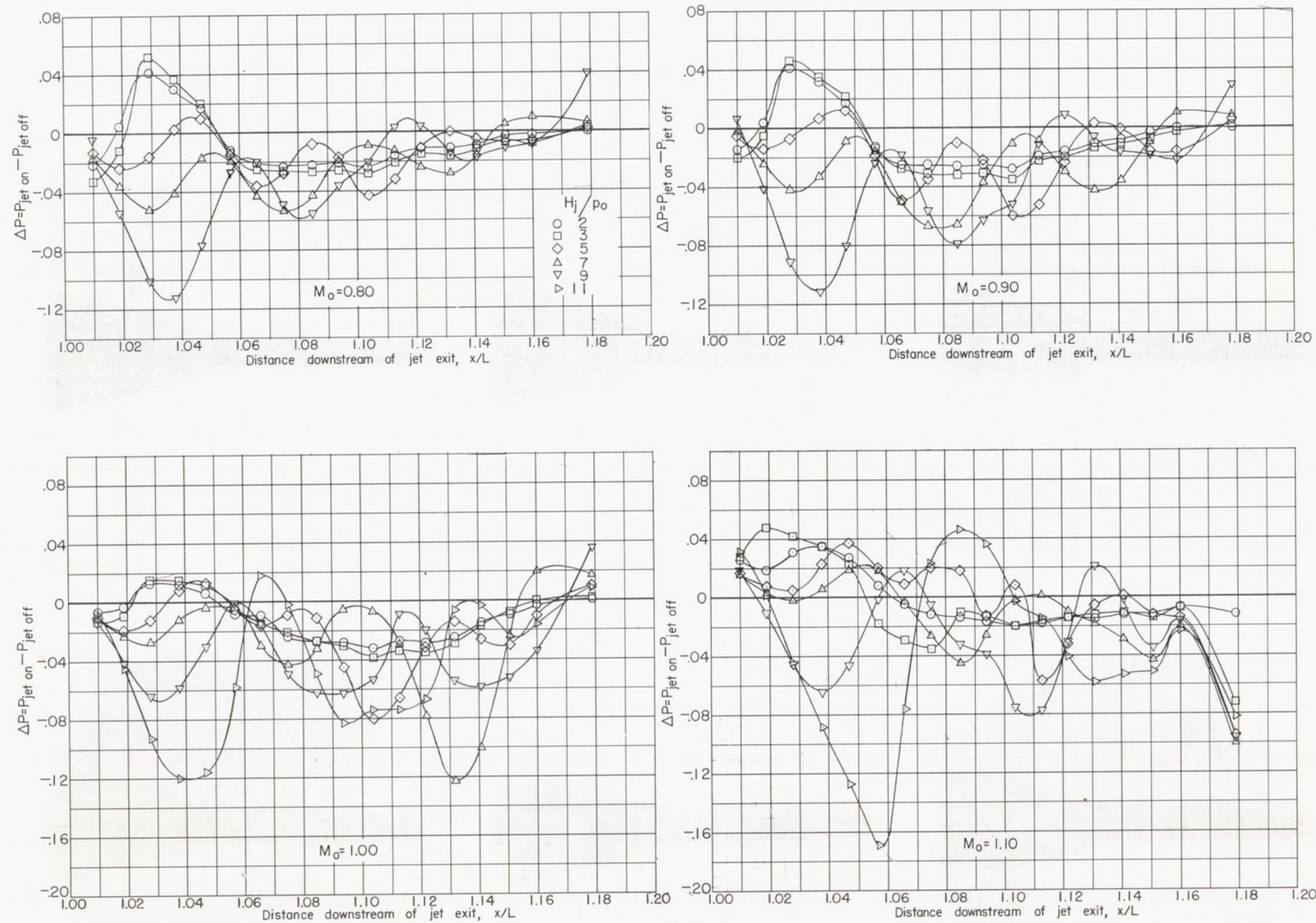
(a) $\phi = 7^\circ$; $h/D_j = 0.855$; $M_0 = 0.80$ and 0.90 .

Figure 9.- Effect of jet operation on pressure distribution along fuselage overhang. $T_j = 1,200^\circ F.$



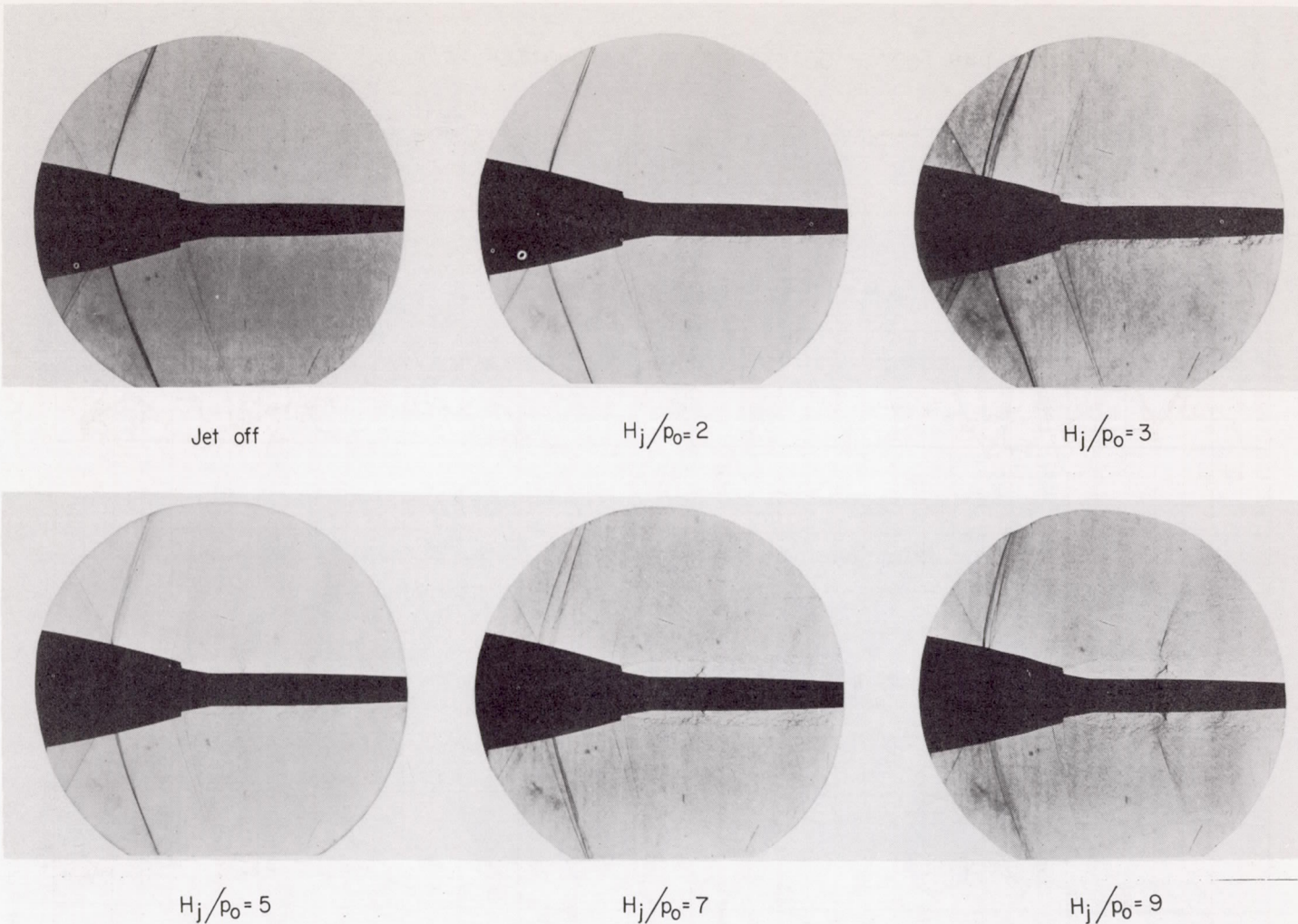
(b) $\phi = 7^\circ$; $h/D_j = 0.855$; $M_0 = 1.00$ and 1.10 .

Figure 9.- Continued.



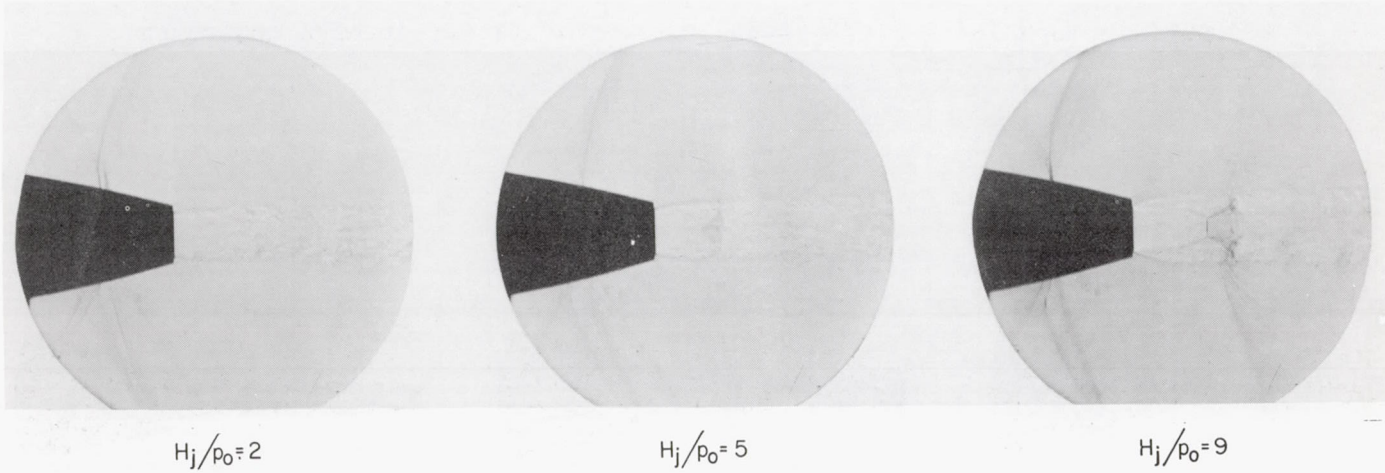
(c) $\phi = 7^\circ$; $h/D_j = 1.040$; $M_0 = 0.80, 0.90, 1.00$, and 1.10 .

Figure 9.- Concluded.

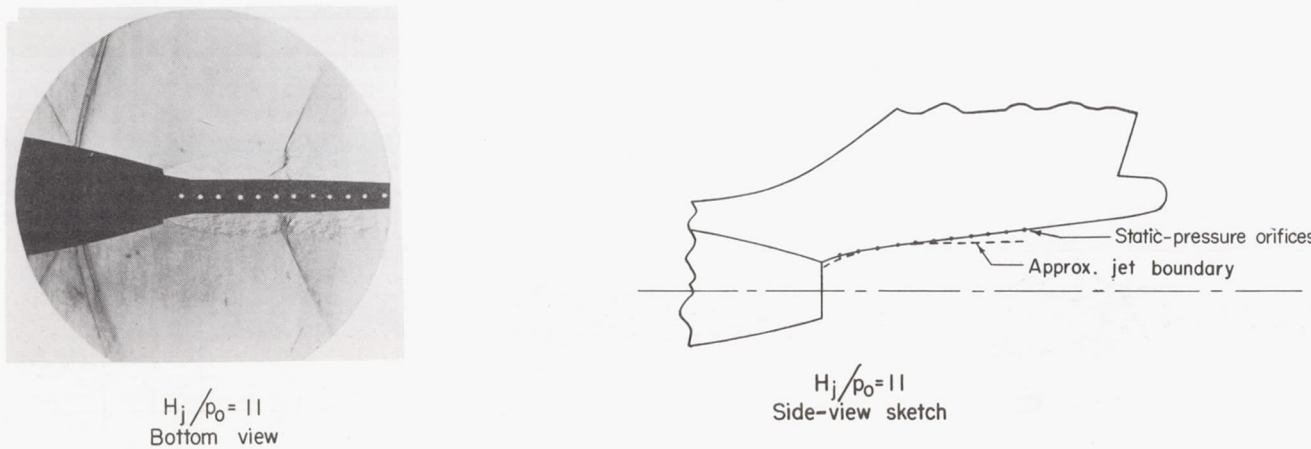


(a) Bottom view of jet in presence of overhang ($\phi = 7^\circ$; $h/D_j = 0.855$). L-91757

Figure 10.- Schlieren photographs illustrating jet structure. $M_\infty = 1.10$;
 $T_j = 1,200^\circ \text{ F.}$



(b) View of jet in absence of overhang.



(c) Sketch illustrating jet attachment to overhang surface.

L-91758

Figure 10.- Concluded.

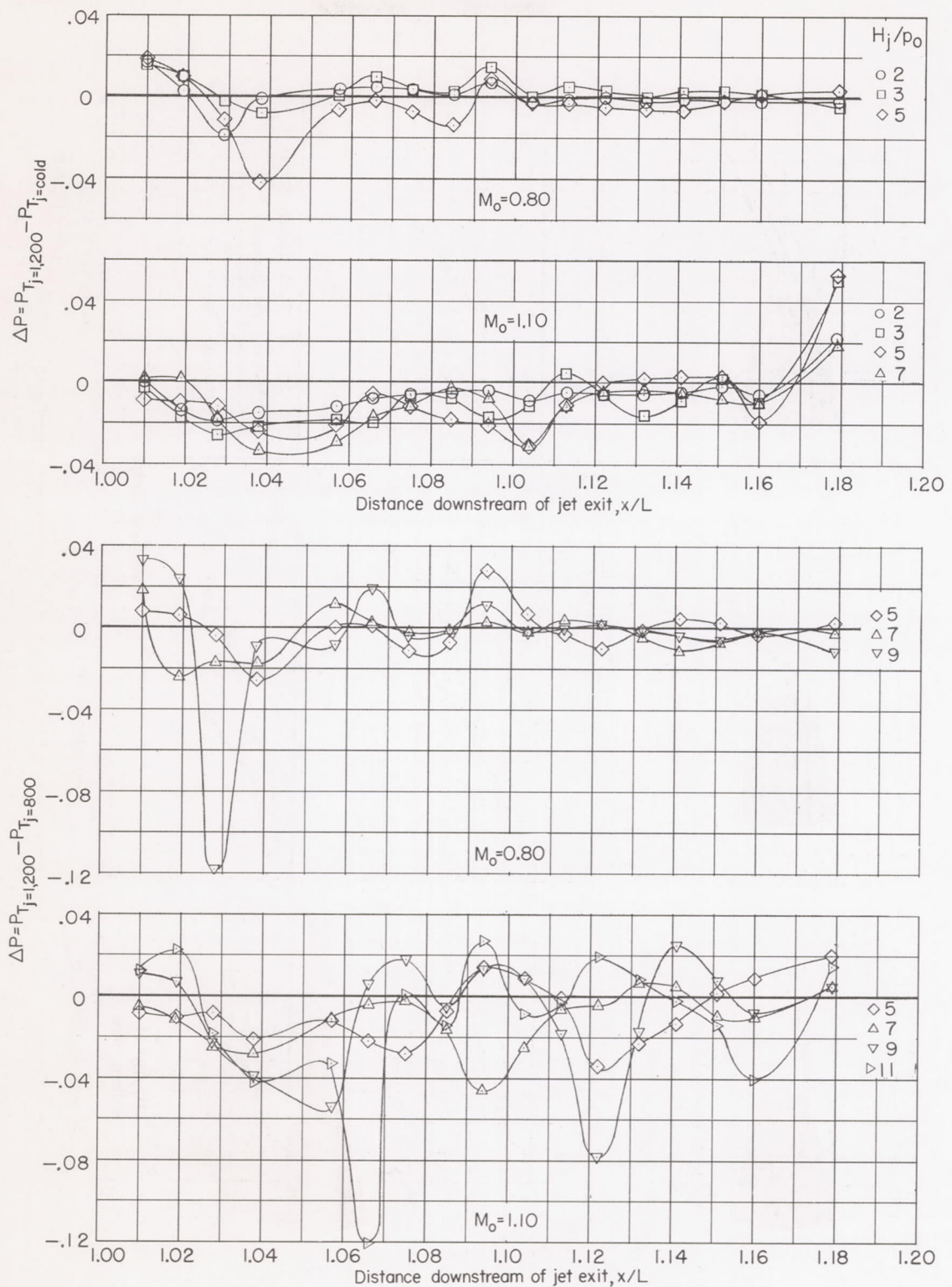


Figure 11.- Effect of jet temperature on pressure distribution along fuselage overhang. $\phi = 7^\circ$; $h/D_j = 0.855$.

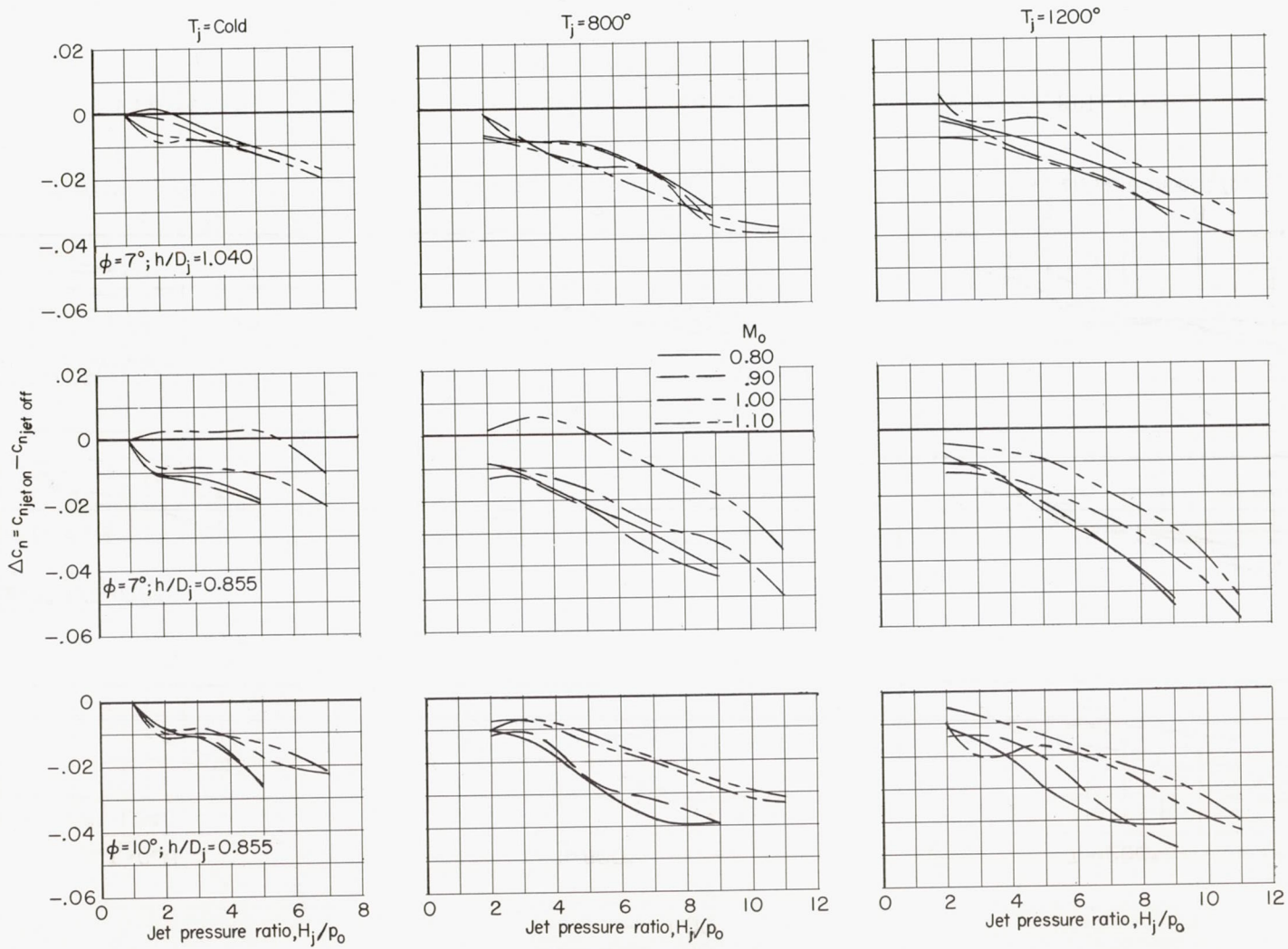


Figure 12.- Variation of increment in section normal-force coefficient with jet pressure ratio.

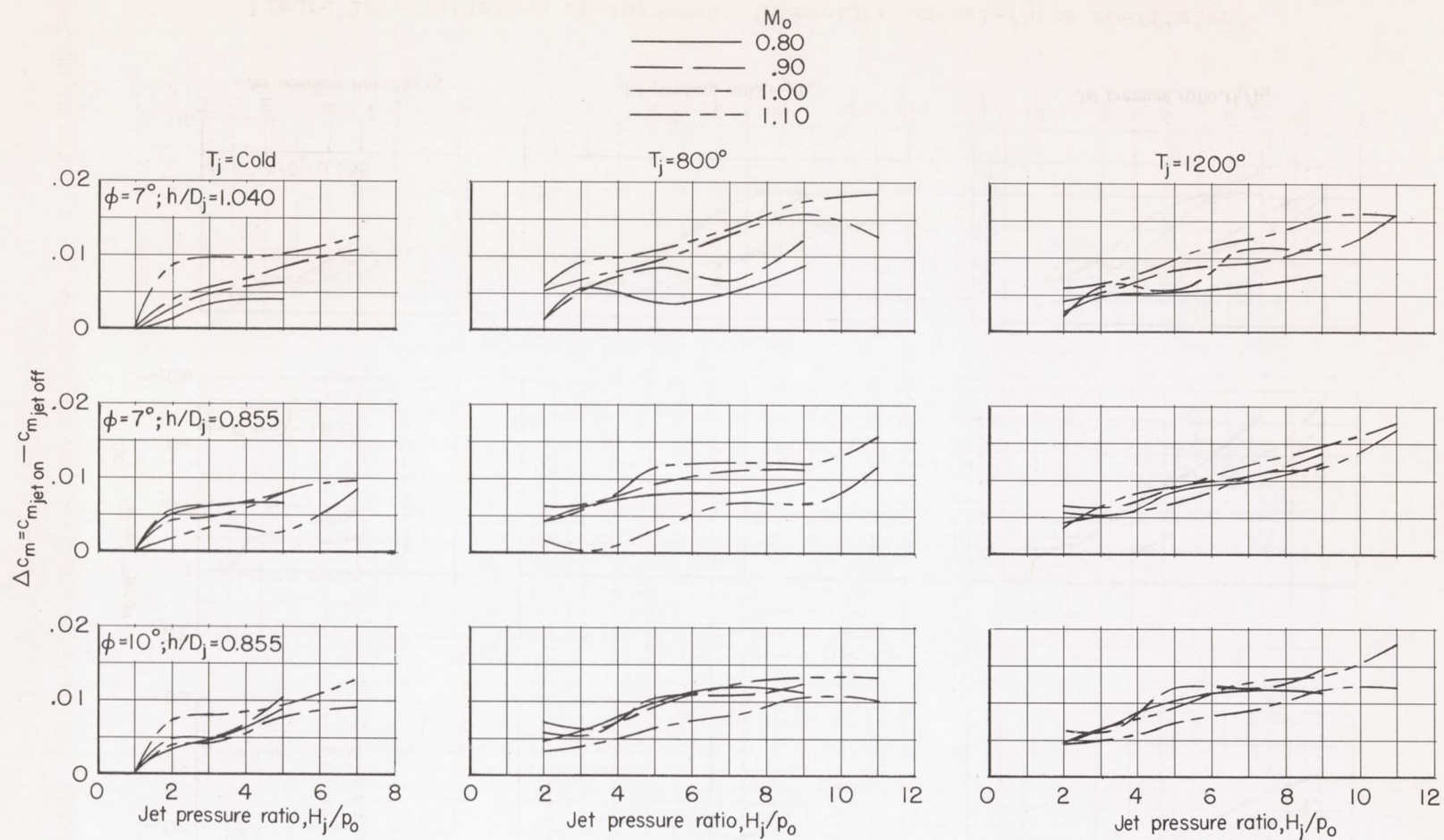


Figure 13.- Variation of increment in section pitching-moment coefficient with jet pressure ratio.

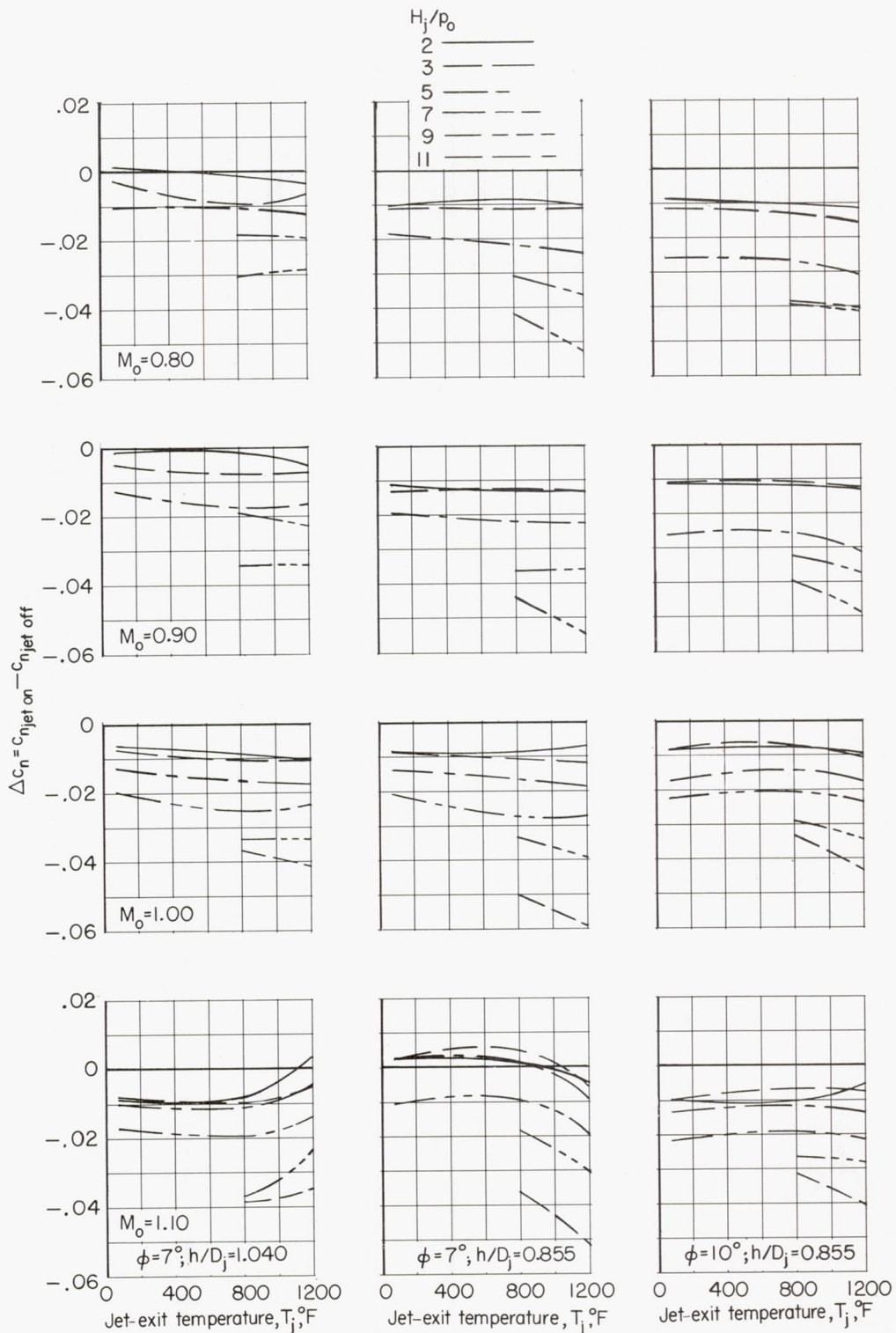


Figure 14.- Effect of jet-exit temperature on increment in section normal-force coefficient due to jet.

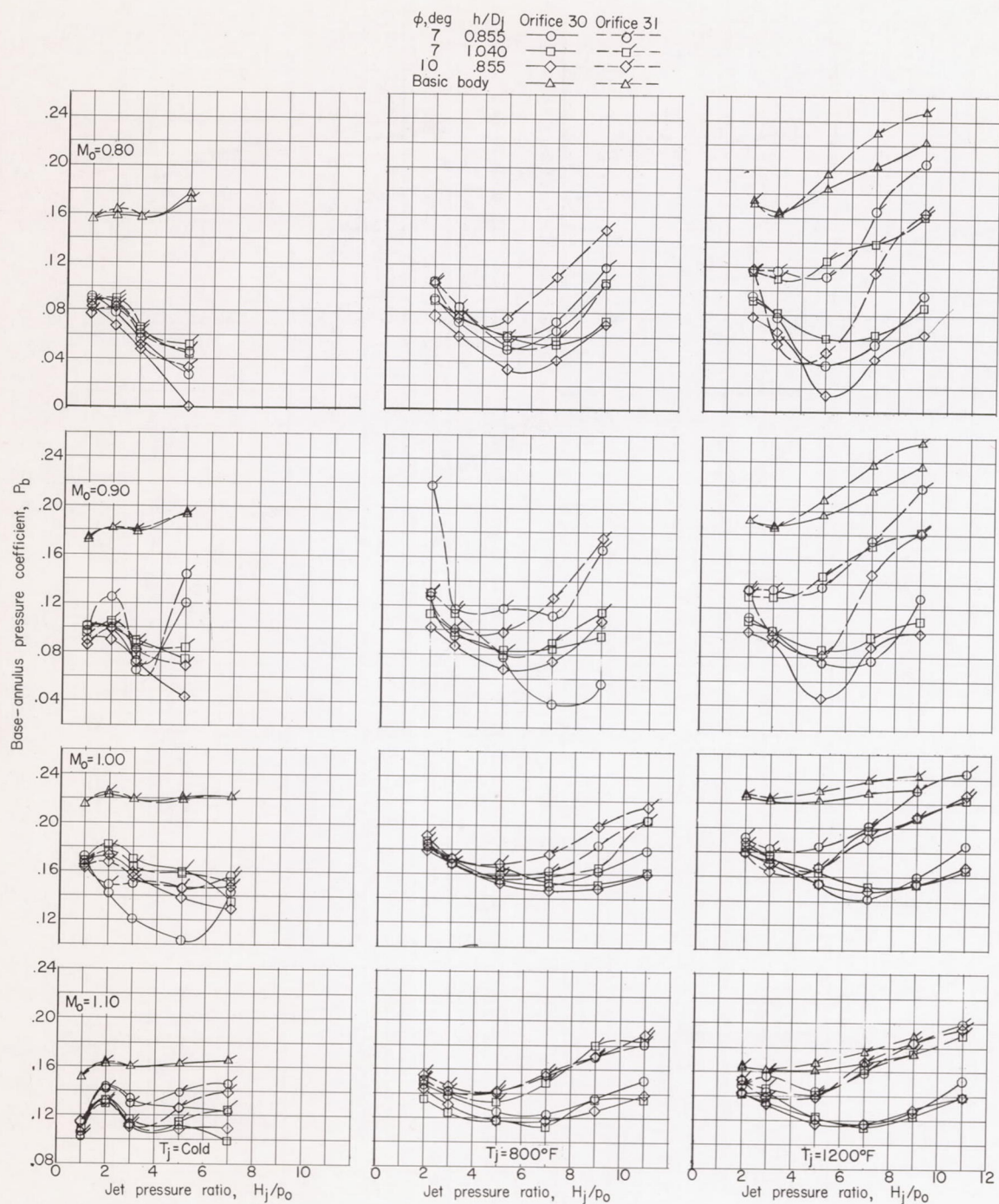


Figure 15.- Effect of jet pressure ratio and fuselage-overhang geometry on base-annulus pressure coefficient.

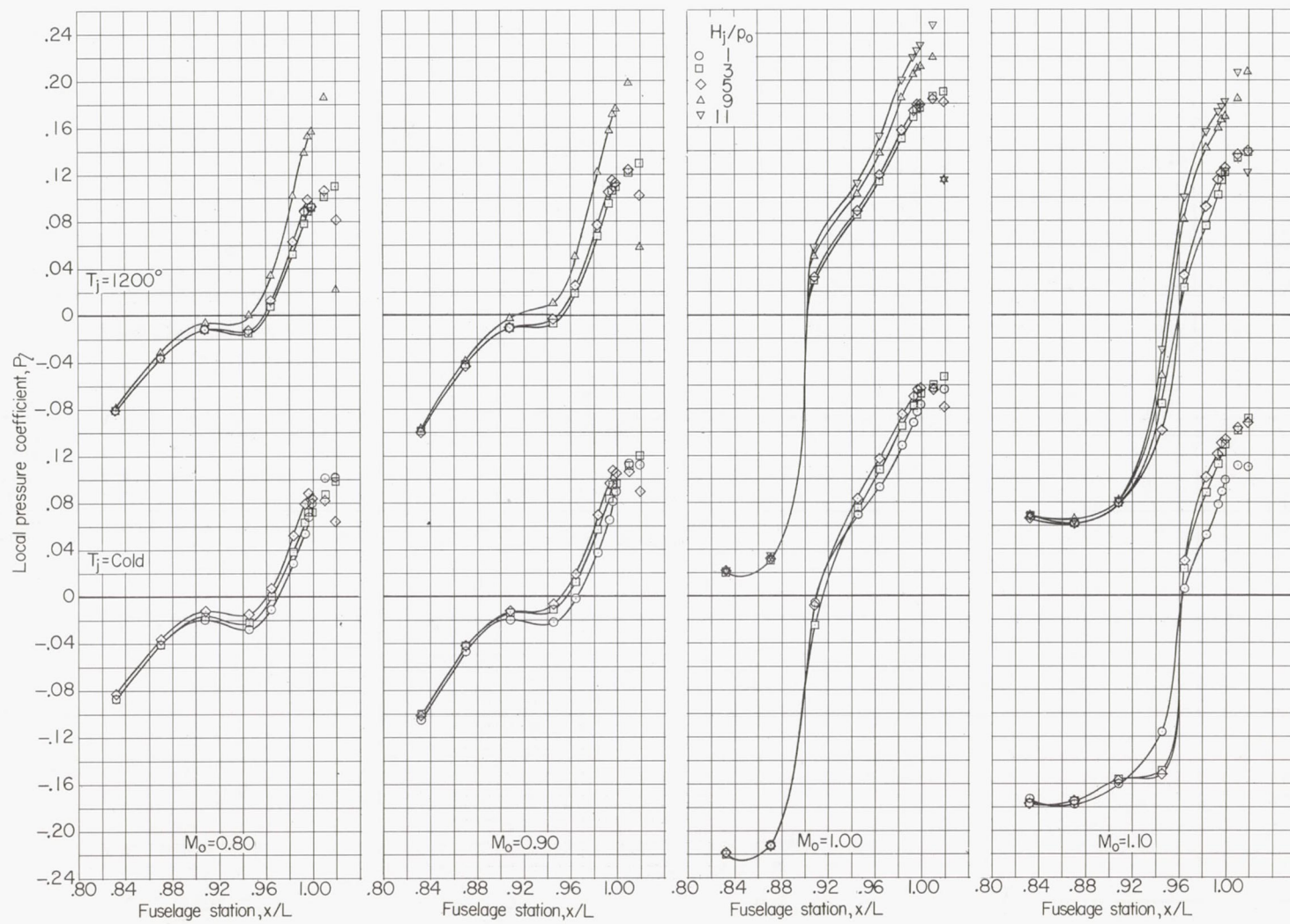


Figure 16.- Effect of jet-on pressure distribution upstream of jet exit.
 $\phi = 7^\circ$; $h/D_j = 0.855$.